



# VCU

Virginia Commonwealth University  
VCU Scholars Compass

---

Theses and Dissertations

Graduate School

---

2015

## The Role of tfec in Zebrafish Neural Crest Cell and RPE Development.

Samantha A. Spencer  
*Virginia Commonwealth University*

Follow this and additional works at: <https://scholarscompass.vcu.edu/etd>



Part of the [Genetics Commons](#)

© The Author

---

Downloaded from

<https://scholarscompass.vcu.edu/etd/3754>

This Thesis is brought to you for free and open access by the Graduate School at VCU Scholars Compass. It has been accepted for inclusion in Theses and Dissertations by an authorized administrator of VCU Scholars Compass. For more information, please contact [libcompass@vcu.edu](mailto:libcompass@vcu.edu).

**© 2015 Samantha Ashley Spencer**  
All rights reserved

# The role of *tfec* in zebrafish neural crest cell and rpe development.

A thesis submitted in partial fulfillment of the requirements for the degree of  
Master of Science at Virginia Commonwealth University

By  
Samantha Ashley Spencer  
Bachelor of Science, Virginia Commonwealth University, 2013

Director: James A Lister, PhD  
Assistant Professor  
Department of Human and Molecular Genetics

Virginia Commonwealth University  
Richmond, Virginia  
April, 2015

## **Acknowledgement**

I first would like to thank Dr. Jim Lister for his continuous support and patience throughout this project. His kind words and many jokes have made the last two years lighthearted and fun, and have made working in his lab an enjoyable experience. Furthermore, his relaxed approach with regards to my experiments gave me room to grow as a scientist and develop my skills as a researcher, for which I am grateful.

I also would like to thank the members of my committee, Dr. Joyce Lloyd, for the invaluable help with my academic pursuits and the professional advice regarding my thesis and career, and Dr. Gregory Walsh, whose additional insight into zebrafish research has aided my experiments.

Additional thanks are needed for the members of my lab, Josh, Thao, Lauren and Natalie, and others here for a short while, for the laughs and support throughout this endeavor.

Many thanks to my boyfriend Nav, whose endless patience and additional expertise has undeniably aided in the completion of my thesis. I must also thank my family, especially my parents, for their kind words and constant encouragement throughout this project.

Finally, I would like to thank my sister, Lea, whose beautiful mind has sparked this entire journey of academic discovery.

## Table of Contents

	Page
Acknowledgment.....	ii
List of Tables and Figures.....	vii
List of Abbreviations.....	ix
Abstract.....	xi
CHAPTERS:	
1. INTRODUCTION.....	1
a. Pigmentation.....	1
b. Pigment cells.....	1
c. Pigmentation of the skin, hair and irises.....	2
d. The vertebrate eye.....	4
e. Zebrafish as a model organism.....	7
f. Neural crest cell development.....	8
g. Eye development.....	15
h. Transcriptional regulation of pigment cell development.....	19
i. Paired homeobox family (PAX).....	19
ii. <i>PAX3</i> .....	19

iii.	<i>PAX6</i> .....	20
iv.	MiT family.....	20
v.	<i>MITF</i> .....	21
vi.	<i>TFEC</i> .....	22
vii.	Interactions of PAX, MITF and TFEC.....	23
i.	Hypothesis and aims.....	24
2.	MATERIALS AND METHODS.....	25
a.	Zebrafish culture and maintenance.....	25
b.	Generating <i>tfec</i> mutations.....	25
i.	Screening potential founder fish.....	26
ii.	PCR.....	26
iii.	TOPO Cloning (Invitrogen protocol) and Transformation.....	27
iv.	Fin clipping for genotyping.....	28
c.	Genotyping the <i>mitfa<sup>w2</sup>;tfec</i> double mutants.....	28
d.	Morpholino injections.....	29
e.	CRISPR/Cas9 injections.....	29
f.	In situ hybridization (ISH).....	30
3.	RESULTS.....	32
a.	Sequencing of TALEN-derived and CRISPR-derived mutants.....	32
i.	Exon 8.....	33
ii.	Exon 3.....	34
iii.	Exon 7.....	37

b.	<i>tfec</i> morphants and mutants show delayed pigmentation and rpe development.....	39
i.	<i>tfec</i> mutants and morphants show delayed eye melanogenesis.....	42
ii.	<i>tfec</i> mutants show reduced expression of markers for rpe.....	44
iii.	<i>tfec</i> mutants have reduced eye size.....	45
iv.	<i>tfec</i> mutants and morphants show delayed xanthophore pigmentation.....	47
v.	<i>tfec</i> mutants show a loss of iridophores.....	50
vi.	<i>tfec</i> mutations disrupt the organization of trunk melanophores.....	52
c.	<i>tfec;mitfa</i> double mutants lose pigmentation in neural crest and rpe.....	54
i.	<i>tfec;mitfa</i> double mutants have abnormal eye shapes.....	54
ii.	<i>tfec;mitfa</i> double mutants and morphants show a greater loss of eye melanogenesis.....	56
iii.	Double mutants show a greater loss of rpe.....	58
iv.	<i>tfec;mitfa</i> double mutants show reduced eye and head size.....	59
v.	Double mutants lose xanthophore pigmentation.....	60
vi.	<i>tfec;mitfa</i> double mutants show a loss of iridophores.....	63
d.	Phenotype of exon 8 TALEN-derived mutants.....	65
e.	Genotyping of exon 3 TALEN-derived mutants.....	65
4.	DISCUSSION.....	66
a.	Pigmentation regulation in zebrafish.....	66
b.	Zebrafish as pigment cell and eye development models.....	67
c.	Regulation of pigment cell development.....	68
d.	Establishment of several mutant lines for <i>tfec</i> .....	69

e. <i>tfec</i> positively regulates development of iridophores, xanthophores and <i>rpe</i> .....	70
f. <i>tfec</i> and <i>mitfa</i> cooperatively regulate <i>rpe</i> , iridophore and xanthophore development..	72
g. Conclusions.....	74
Literature Cited.....	77
Vita.....	86

## List of Tables and Figures

	Page
Figure 1. Pigment patterns of the adult and embryonic zebrafish.....	3
Figure 2. Sagittal section of the human eye.....	5
Figure 3. The retinal pigment epithelium (rpe) in visual function.....	6
Figure 4. Neural keel and neural tube formation in zebrafish.....	9
Figure 5. Diagram representing the migration pathways of the chromatoblasts of mouse, chick and zebrafish.....	12
Figure 6. Embryonic pigmentation pattern including labeling of the four melanophore stripes.....	14
Figure 7. Formation of the optic cup.....	17
Table 1. Primer sequences used in this study.....	27
Table 2. Expected product sizes of PCR and subsequent digestion where applicable.....	27
Figure 8. Diagram of exon 8 of <i>tfec</i> .....	35
Figure 9. Sequences of mutants in exon 8 of <i>tfec</i> .....	35
Figure 10. Diagram of exon 3 of <i>tfec</i> .....	36
Figure 11. Sequencing results of TALEN-derived <i>tfec</i> exon 3 mutants.....	37
Figure 12. Diagram of the binding site for the CRISPR guideRNA for exon 7.....	38
Figure 13. Sequences of several <i>tfec</i> exon 7 mutants.....	39

Table 3. Number of in situ hybridizations for each marker, background and timepoint.....	41-42
Figure 14. Delayed eye melanogenesis and growth in <i>tfec</i> mutants.....	43
Figure 15. Morphant embryos for <i>tfec</i> show a delayed expression of <i>dct</i> .....	43
Figure 16. Delayed expression of <i>pmelb</i> in eyes of <i>tfec</i> mutant embryos.....	44
Figure 17. Eye areas of control and CRISPR-injected embryos.....	46
Figure 18. Xanthophore pigmentation is delayed in <i>tfec</i> mutants.....	48
Figure 19. Morphant embryos for <i>tfec</i> show loss of expression of <i>xdh</i> .....	48
Figure 20. Delayed expression of <i>fms</i> in <i>tfec</i> morphants and mutants.....	49
Figure 21. Loss of iridophores in <i>tfec</i> CRISPR-injected embryos.....	51
Figure 22. <i>tfec</i> mutants show reduced expression of <i>ltk</i> .....	51
Figure 23. Loss of <i>tfec</i> disrupts melanophore organization.....	53
Figure 24. Double mutants show non-circular ocular globes.....	55
Figure 25. Double mutants show delayed melanogenesis with loss of melanin in the medial retina and delayed choroid fissure closure.....	57
Figure 26. Double mutants show delayed <i>dct</i> expression with a loss of expression from the medial retina.....	57
Figure 27. Double mutants show loss of <i>pmelb</i> expression.....	58
Figure 28. Eye sizes of CRISPR-injected and control embryos in <i>mitfa</i> mutant background.....	59
Figure 29. Loss of xanthophore pigmentation in <i>tfec</i> mutants.....	61
Figure 30. Loss of <i>xdh</i> expression in double mutants.....	61
Figure 31. Loss of <i>fms</i> expression in double mutants.....	62
Figure 32. Loss of iridophores in double mutants.....	64

Figure 33. Reduced expression of *ltk* in double mutants.....64

Figure 34. Model of the roles of *mitfa* and *tfec* in pigment cell differentiation.....76

### List of Abbreviations

A/M – Anophthalmia/microphthalmia

BCIP - 5-bromo-4-chloro-3'-indolylphosphate p-toluidine salt

BMP - Bone morphogenetic protein

BSA - Bovine serum albumin

Cas9 – CRISPR-associated protein 9

CRISPR - Clusters of regularly interspaced short palindromic repeats

DCT – Dopachrome tautomerase

DNA - Deoxyribonucleic acid

DPF - Days post fertilization

FMS - colony stimulating factor 1 receptor a

HPF - Hours post fertilization

Hyb - Hybridization buffer

IHC - Immunohistochemistry

ISH - In situ hybridization

LTK - Leukocyte tyrosine kinase

MeOH - Methanol

MESAB - Ethyl 3-aminobenzoate, methanesulfonic acid salt 98%

MiT – Microphthalmia/Transcription Factor E

MITF – Microphthalmia-associated transcription factor

MO - Morpholino

NBT - Nitro blue tetrazolium chloride

NHEJ - Non-homologous end joining

OTX – Orthodenticle homeobox

PAX – Paired homeobox

PBS - Phosphate Buffered Saline ix

PBT - PBS + 0.05% Tween-20

PCR - Polymerase Chain Reaction

PFA - Paraformaldehyde

PMELB - Premelanosome protein B

RPE - Retinal Pigmented Epithelium

RT - Room Temperature

RVD - Repeat variable diresidues

SSC - Sodium citrate buffer

TALEN - Transcription activator-like effector nucleases

TFEC – Transcription factor EC

XDH – Xanthine dehydrogenase

ZIRC - Zebrafish International Resource Center

## Abstract

### THE ROLE OF *TFEC* IN ZEBRAFISH NEURAL CREST CELL AND RPE DEVELOPMENT

Samantha Ashley Spencer, B.S.

A thesis submitted in partial fulfillment of the requirements for the degree of Master of Science at Virginia Commonwealth University.

Virginia Commonwealth University, 2015

Major Director: James A. Lister,  
Assistant Professor, Department of Human and Molecular Genetics

Zebrafish (*Danio rerio*) show a unique pigmentation pattern comprised of three pigment cell types: melanophores, iridophores and xanthophores. Other pigmented cells include the retinal pigmented epithelium (rpe) which absorbs excess light in the eye and maintain the extracellular environment around the photoreceptors. While previous mutations in *mitfa* showed a role in regulating trunk melanophores, the rpe was not affected. TALENs and CRISPR-Cas9 systems were used to generate mutant zebrafish for *tfec*, a transcription factor expressed in both neural crest and rpe. Embryos with *tfec* mutations showed a loss of iridophore pigmentation, and delays in the pigmentation of xanthophores and rpe, showing positive regulation of multiple pigment cells. Double mutants for *tfec* and *mitfa* displayed greater losses of iridophore, xanthophore and rpe pigmentation with noncircular globes, suggesting cooperative roles for these transcription factors.

## **CHAPTER 1: INTRODUCTION**

### **Pigmentation**

Pigmentation within an organism serves a variety of functions toward survival. Darker skin pigment in humans protects against UV radiation, preventing damage of the DNA within skin epidermal cells (Alaluf et al, 2002). Pigmentation in mice and many other animals provides camouflage by allowing those organisms to blend in with their surroundings; for example beach mice have lighter fur pigment than their mainland counterparts (Steiner et al, 2008). Finally, pigmentation may be sexually dimorphic and therefore important for mating.

### **Pigment cells**

The primary mammalian pigment, melanin, is produced in organelles called melanosomes (Lin and Fisher, 2007). Melanin can be further divided into two types: yellow/red pheomelanin and brown/black eumelanin. Both types of melanin are derived from the precursor tyrosine via the enzyme tyrosinase (TYR), which converts tyrosine to dopaquinone. Tyrosinase-related protein 1 (TYRP1) and TYRP2, also known as dopachrome tautomerase (DCT), convert dopaquinone to eumelanin. Pheomelanin is derived from conjugation of dopaquinone with thiols such as cysteine or glutathione. All pigment cells produce melanin in melanosomes, specialized organelles that separate the photoreactions important in the function of pigmentation from the rest of the cell (Cichorek et al, 2013). Each melanin-

producing tissue maintains differing numbers of melanosomes in different stages of development.

Teleosts contain three types of pigment cells called chromatophores (Quigley and Parichy, 2002). Each chromatophore produces a different type of pigment: melanophores, analogous to melanocytes; xanthophores which contain a yellow pteridine pigment; and iridophores which contain iridescent purine platelets (Figure 1). Melanophores also contain melanosomes where melanin is produced, and the other pigment cells have similar structures to store their respective pigments.

### **Pigmentation of the skin, hair and irises**

Melanocytes are the pigment-producing cell in the skin, hair and irises of the eye in mammals. Melanocytes produce melanin in melanosomes, which are then passed to neighboring keratinocytes where the majority of pigment is stored as supranuclear caps (Cichorek et al, 2013; Lin and Fisher, 2007). The color of human skin is primarily determined by amounts of eumelanin. Hair pigmentation is a result of variation of levels of both eumelanin and pheomelanin (Cichorek et al, 2013). Hair keratinocytes contain larger, more mature melanosomes that are degraded less than in the skin. Surrounding the pupil is the colored circular muscle, the iris that contracts and dilates the pupil in different light levels (Kolb et al, 2012). Iris color is determined by melanocytes in the uveal tract, or the anterior portion of the iris (Sturm et al, 2004). All eyes contain similar numbers of melanocytes; brown eyes contain many melanosomes with dense melanin pigment, whereas blue eyes contain little melanin. Unlike within the skin and hair, melanosomes are not transported to neighboring cells, but instead accumulate in the cytoplasm of the melanocyte.

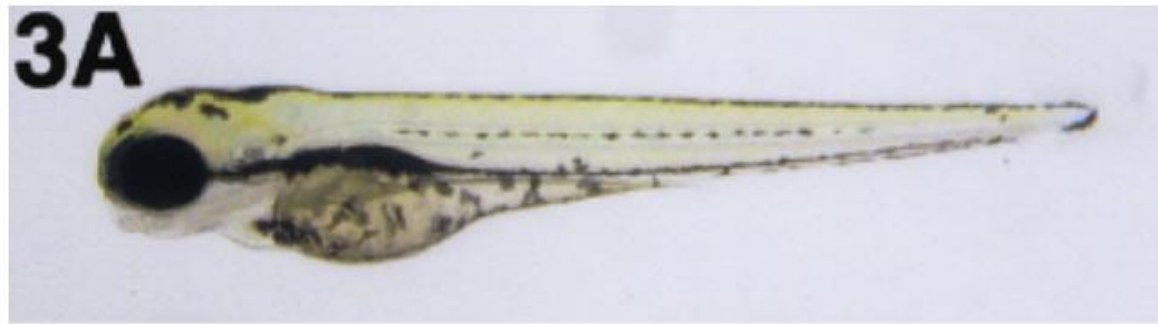
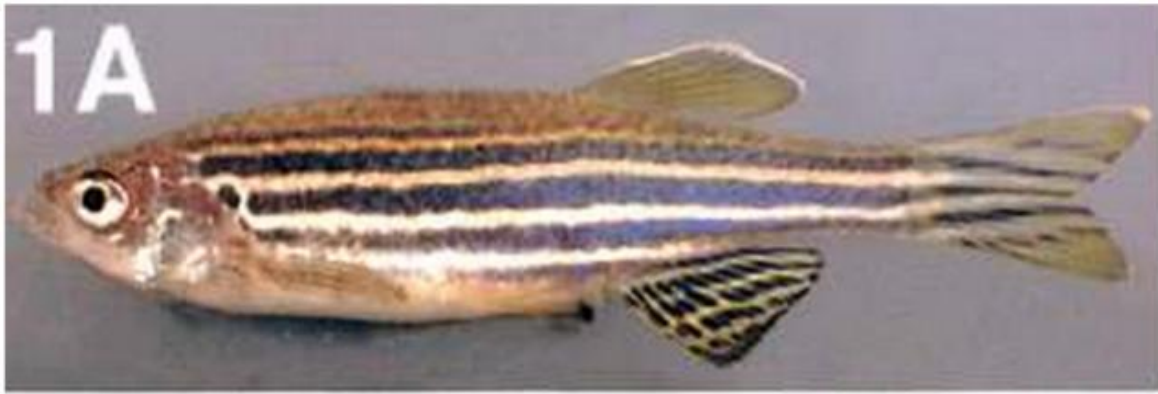


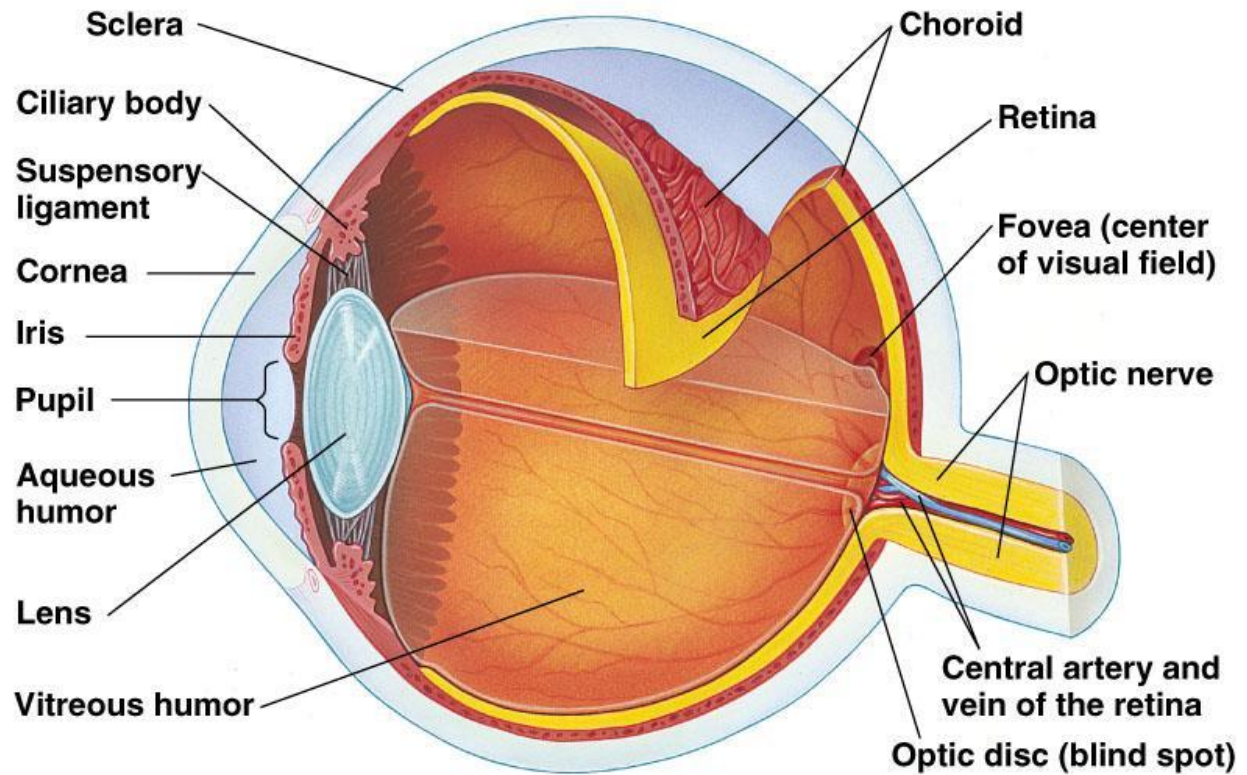
**Figure 1. Pigment patterns of the adult and embryonic zebrafish.** Top: Adults typically have 4-5 dark melanophore stripes and lighter yellow xanthophore stripes. All of the stripes are covered with iridescent cells called iridophores, giving zebrafish an all-over sheen. Bottom: Embryos show a different pigmentation pattern comprised of the same pigment cells as in the adult. The metamorphosis between the two patterns occurs around 2 weeks after fertilization. Iridophores are not visible because transmitted light is used rather than incident light. (Quigley and Parichy, 2002)

Teleosts have chromatophores in the dermis and in the eye (Quigley and Parichy, 2002). The chromatophores within the skin give rise to the striped pattern for which zebrafish are named where melanophores and xanthophores alternate, eventually forming 4-5 dark stripes in the fully grown adult (Figure 1). Iridophores are seen in both dark and light stripes, giving a pearlescent appearance to the light stripes and a iridescent blue hue to the dark stripes. Teleosts do not have irises, which are muscles in mammals meant to focus light onto the lens; however, a circular pattern of iridophores and melanophores are present on the eye surface. The pigment containing organelles remain within the chromatophores rather than being transferred to neighboring cells as in other species.

### **The vertebrate eye**

Light passes through the pupil, lens and vitreous humor to reach the back of the eye where the retina is located (Figure 2) (Kolb et al, 2012). The retina is comprised of layers of cells with different functions in vision. The neural layer farthest from pupil is the photoreceptors; humans have one type of rod that perceives low-level light and three cones that respond to different wavelengths of light corresponding to the colors red, green and blue.

The retinal pigment epithelium (rpe) lies behind the photoreceptors (Figure 3) (Kolb et al, 2012). Excess light not absorbed by the photoreceptors is absorbed by the melanin within the melanosomes of the rpe (Wasmeier et al, 2008). Skin melanocytes constantly produce additional melanin; however, in the rpe, melanin production is finished in mouse *in utero*, and the pigment granules packaged in the melanosomes will remain for life (Kolb et al, 2012). Degradation by photooxidative damage of the rpe is thought to contribute to decline in vision in aging people, specifically macular degeneration.



Copyright © Pearson Education, Inc., publishing as Benjamin Cummings.

Figure 2. Sagittal section of the human eye. (Kolb et al, 2012)

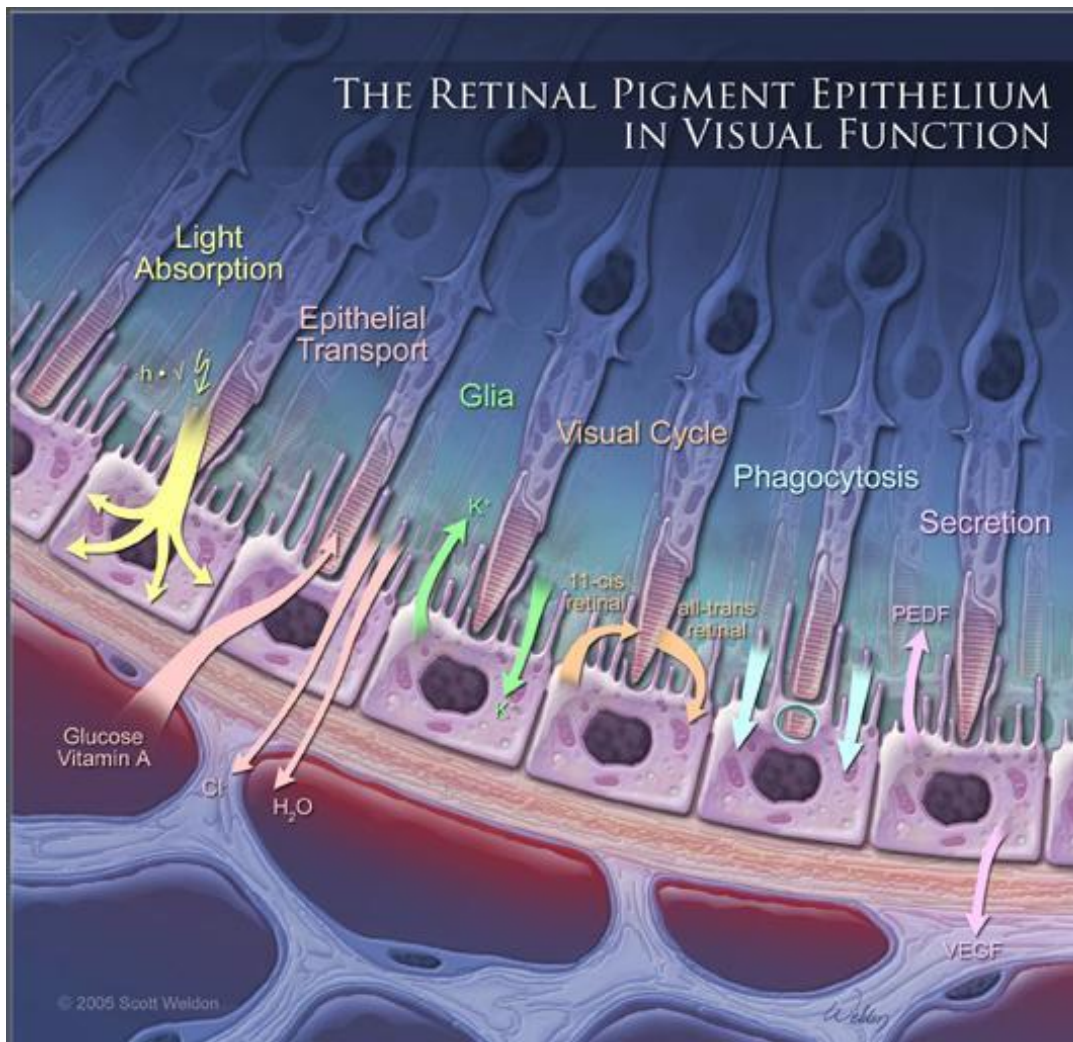


Figure 3. The retinal pigment epithelium (rpe) in visual function. © Scott Weldon 2005.

Opsins are G protein-coupled receptors in rods and cones that contain 11-cis-retinal; when opsins absorb a photon, the GPCR changes conformation and converts 11-cis-retinal to trans-retinal, which is then released out of the cell (Kolb et al, 2012). The conversion of trans-retinal to 11-cis-retinal is critically important in visual function; the rpe contains the enzymes responsible for this process. Over time, the photoreceptor outer segments (POS) which absorb photons become photodamaged, and are shed from the photoreceptors at a constant rate. Photodamaged portions are phagocytosed by the rpe at a rate similar to their shedding from the photoreceptors.

The rpe also maintains the extracellular environment of the retina by uptaking ions, such as potassium and calcium, or the photoreceptor neurotransmitter, glutamate (Kolb et al, 2012). The choroid, a layer of vasculature located behind the rpe, provides glucose which undergoes glycolysis in the rpe to yield pyruvate before being passed to the photoreceptors. The rpe also maintains the eye's immune privilege by creating a mechanical barrier between the vasculature and the retina while also sending communication signals such as interleukins to both the bloodstream and the retina. Finally, the rpe secretes extracellular survival signals to the retina such as pigment epithelium-derived factor (PEDF) and fibroblast growth factors (FGFs).

### **Zebrafish as a model organism**

Zebrafish (*Danio rerio*) are well suited for developmental research for multiple reasons. Matings of zebrafish can produce hundreds of transparent embryos that develop *ex utero*, allowing them to be studied during early development (Bibliowicz et al, 2012).

Furthermore, collection at the one-cell stage allows the embryos to be manipulated with

various biotechnologies and chemical treatments. Also, the zebrafish is a vertebrate with more similar physiology to humans than invertebrates like *Drosophila* or *C elegans*.

### **Neural crest cell development**

Neural crest cells are formed during neurulation, and migrate and differentiate after neural tube formation. Neural crest development can be divided into four stages: induction, delamination, migration and differentiation.

Neurulation is the process by which the neural tube forms, which will eventually become the brain and spinal cord. This process begins with two tissues: the ectoderm and the notochord (Purves et al, 2001). The notochord secretes signaling molecules, including fibroblast growth factors (FGFs) and bone morphogenic protein (BMP), that causes the cells of the ectoderm to become an epithelial layer, forming the neural plate (Basch et al, 2004). These cells thicken along the basal side and cause the neural plate to form a horseshoe (Colas and Schoenwolf, 2001). Hinge cells near the notochord and on either side of the presumptive neuroectoderm, within the neural grooves, help to form this shape by keeping some cells tethered while the rest of the tissue layer moves. As the number of cells increase, the neural grooves eventually meet and fuse, forming the neural tube. The entire neural tube develops along a rostrocaudal gradient. In zebrafish, neurulation occurs slightly differently; the neural tube forms initially as a neural keel without a lumen and without neural grooves (Figure 4) (Strähle and Blader, 2004). The lumen forms after the neural tube has developed.

The first stage of neural crest cell development is induction of the neural crest. The presumptive neural crest forms at the border of the ectoderm and the presumptive epidermis due to the signaling gradients from the notochord and ectoderm; intermediate levels of FGF

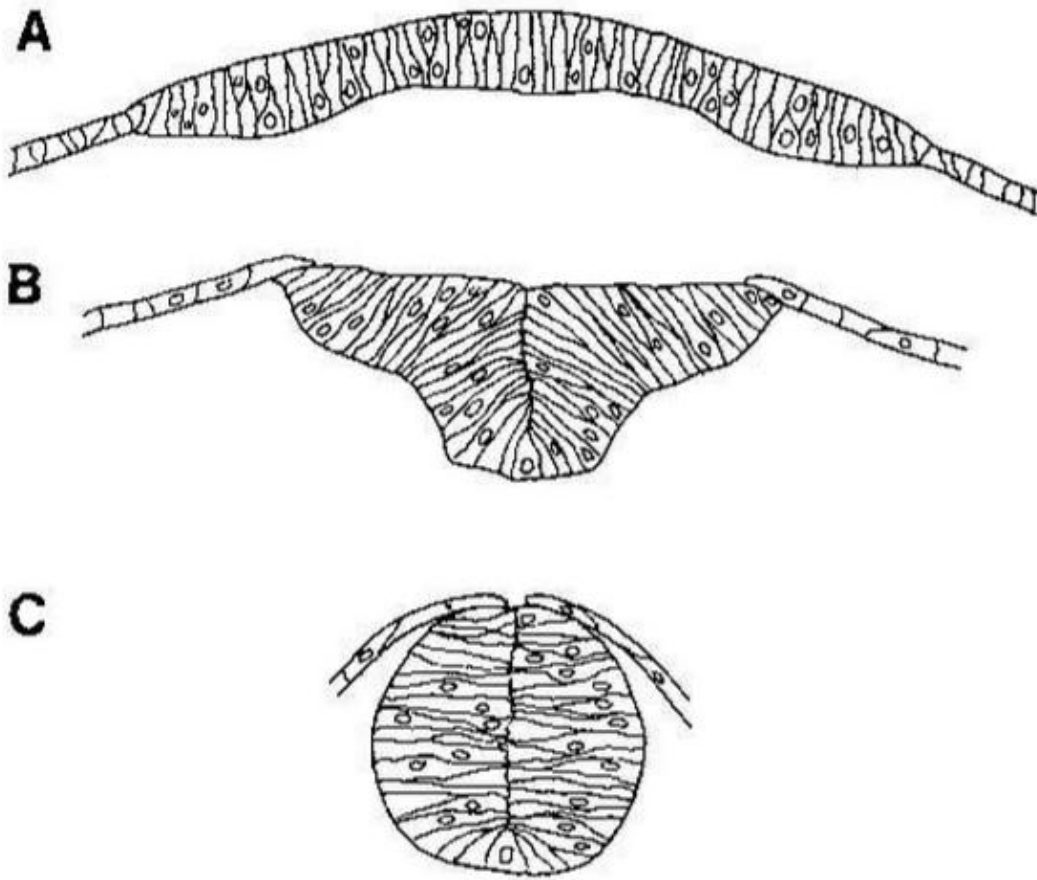


Figure 4. Neural keel and neural tube formation in zebrafish. (Kimmel et al, 1995)

and BMP lead to the development of neural crest (Basch et al, 2004). Continued signaling from the now distinct neuroectoderm and epidermal ectoderm cause the formation of a border zone between these two tissue types which will become the neural crest. As the neural plate begins to bend and reshape, the neural crest is located at the neural grooves, tethered by the hinge cells in that part of the ectoderm (Colas and Schoenwolf, 2001). In the zebrafish neural keel, neural grooves are not present; neural crest cells instead are within the neural keel with no morphological structure to locate them, though using markers can be localized to the dorsal portion (Strähle and Blader, 2004; Eisen and Weston, 1993). As a result of the primary induction by outside signals, these cells begin expressing genes specific to the presumptive neural crest, further restricting these cells' fate. Examples of these genes include *Snail/Slug* family members, *Msx-1* and *Msx-2*, *Sox9* and *10*, and *Pax-3* and *Pax-7*. Expression of these genes can be used as markers to identify presumptive neural crest within the developing neural tube.

Following induction, the presumptive neural crest delaminates from the neural tube. Delamination refers to the separation of one tissue into two separate tissues (Theveneau and Mayor, 2011). This process is distinct from the epithelial-mesenchymal transition (EMT) that must also occur for the cells to be able to migrate to their target locations. For example, in mice the neural crest undergoes EMT prior to delaminating, all of which occurs before neural tube closure, while in *Xenopus* cells delaminate during the beginning stages of neural tube closure, and before EMT occurs. In zebrafish and other species, *Snail/Slug* transcription factors are associated with EMT via the downregulation of E-cadherin (Duband, 2000). Neural crest cells also lose their apicobasal polarity during EMT (Theveneau and Mayor, 2011). The genes

that induce delamination and EMT vary even within an organism, both rostrocaudally and temporally; between organisms, variation exists between genes and their roles in neural crest development.

Once the neural crest cells have separated from the developing neural tube, they must migrate to their target destination. Neural crest cells in the head will form cranial ganglia, cartilage and bones of the face, iris, muscles and exterior structure of the eye, and skin (Theveneau and Mayor, 2011). Other neural crest cells below the ears become cardiac muscle. The neural crest cells in the trunk will become peripheral neurons, Schwann cells and the three types of pigment cells. Trunk neural crest cells in zebrafish begin migrating between the somites and the neural tube along the medial pathway, then after four hours, they begin migrating along the lateral pathway between the epidermis and the somite (Figure 5). Melanoblasts use both the medial and lateral pathways, iridoblasts use only the medial pathway and xanthoblasts use only the lateral pathway (Kelsh et al, 2009). Some pigment cells also migrate dorsally to color the dorsal fin (Theveneau and Mayor, 2011). Evidence exists that some presumptive pigment cells exiting the neural crest are not fate-restricted, but instead become fate-restricted following migration; cells within zebrafish express markers for multiple cell types, suggesting a precursor cell able to become any of the three pigment cell types (Quigley and Parichy, 2002). Once the cellular target has been reached, the cells differentiate into the three pigment cell types, reestablish cell-cell contacts, and begin expressing genes specific to that chromatophore, leading to the pigmentation of the embryo.

Zebrafish show two pigmentation patterns throughout development: an earlier larval pattern and a later adult pigmentation pattern that begins to appear after about 14 days

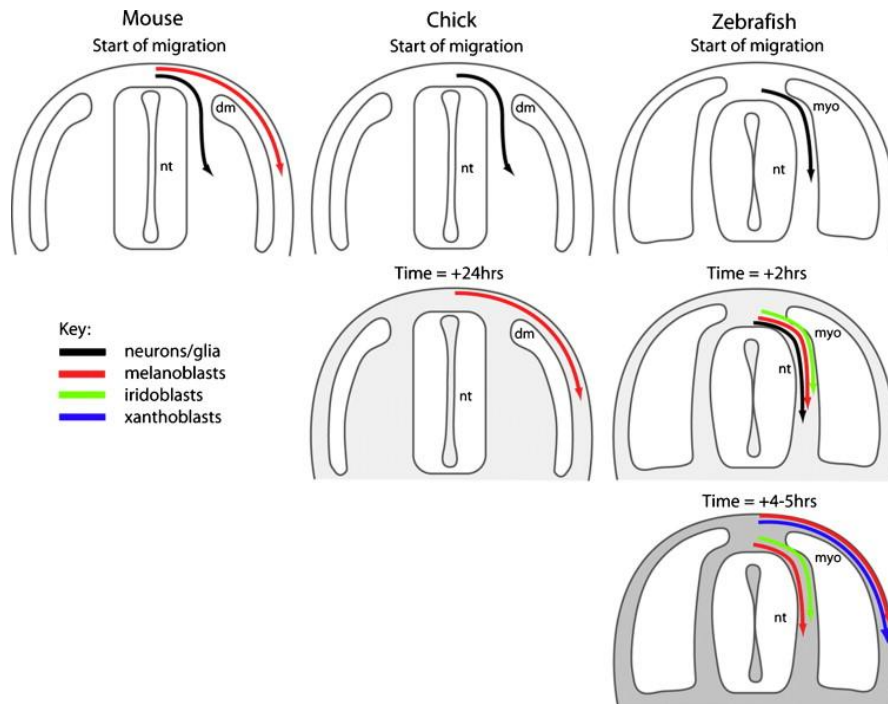


**Figure 5. Diagram representing the migration pathways of the chromatoblasts of mouse, chick and zebrafish.** While pathways for migrating neural crest are similar between species, differences occur in the timing of migration. (Kelsh et al, 2009)

(Quigley and Parichy, 2002). Zebrafish embryos by 3 days old contain four melanophore stripes. These stripes are located as follows: a dorsal stripe from head to tail (DS), a lateral stripe along the horizontal myoseptum (LS), a ventral stripe from between the eyes over the dorsal yolk sack to the tail (VS), and a ventral yolk sac stripe (YSS) (Figure 6) (Kimmel et al, 1995). The iridophores are present along each of the aforementioned melanophore stripes except the lateral stripe. Additionally, embryos have dense patches of melanophores and iridophores present over the swim bladder called lateral patches. Xanthophore pigmentation covers the entire embryo, giving it a yellow hue, especially in the dorsal regions. The metamorphosis between the larval and adult pigmentation patterns is not well understood, but is believed to be a result of subpopulations of chromatophores that, with transcriptional regulation changes, begin being expressed and cause the change in patterning (Quigley and Parichy, 2002).

In humans, mutations in genes affecting neural crest cell development can cause disease with many affected systems. For example, Waardenburg syndrome is a group of diseases caused by mutations in multiple single genes, all affecting the development of neural crest derivatives (Read and Newton, 1997). Individuals with Waardenburg syndrome may have a white forelock, deafness, and pale eyes, sometimes with heterochromia. There are four types of Waardenburg syndrome, each with a slight variation in phenotype. Type 1 shows dystopia canthorum whereas type 2 patients do not. Type 3 patients also have musculoskeletal abnormalities resembling amyoplasia. Type 4 patients experience Hirschsprung's disease in addition to the other Waardenburg symptoms. The different types also reflect mutations in different genes, most of which are inherited in an autosomal dominant fashion with variable



**Figure 6. Embryonic pigmentation pattern including labeling of the four melanophore stripes.** DS=dorsal stripe, LS=lateral stripe, VS=ventral stripe, YSS=yolk sac stripe. Iridophores (not visible) overlay the dorsal, ventral and yolk sac stripes, but not the lateral stripes, and also cover the darkly pigmented eyes and swim bladders. Xanthophores pigment the entire embryo with more yellow pigmentation visible dorsally. (Kelsh et al, 2009)

penetration of each of the symptoms; types 1 and 3 are often caused by mutations in *PAX3*, type 2 by *MITF* mutations, and type 4 by mutations in either *EDN3*, *EDNRB* or *SOX10*.

Zebrafish are beneficial for studying the development of neural crest cells; the *ex utero* fertilization allows early development processes to be studied (Quigley and Parichy, 2002). Neurulation occurs within the first day of development. Furthermore, zebrafish contain more pigment cell types than other vertebrates, and therefore more neural crest cell derivatives. The additional pigment cell types combined with genetic manipulations possible in zebrafish permit a greater study of transcriptional regulation of neural crest development.

### **Eye development**

Eyes appear as optic grooves on either side of the forebrain at day 22 in humans (Gujar and Gandhi, 2011). These grooves evaginate to form the optic vesicles, which invaginate as they approach the surface ectoderm at around 28 days to form the optic cup (Figure 7). The optic cup is a bilayer; the inner layer will develop into the neural retina, and the outer layer will become the rpe. The optic cup is connected to the forebrain via the optic stalk. Around day 32, the surface ectoderm thickens, becoming the lens placode, then pinches off above the optic cup and becomes the lens. As the cup invaginates, a groove forms in the cup called the choroid fissure; the edges of the fissure eventually fuse, creating the round aperture of the pupil. The neural retina differentiates between 6 and 8 weeks of life, and axons from the developing retina extend through the optic stalk to the forebrain, forming the optic nerve. The mesenchymal tissue surrounding the ocular orbit derived in part from neural crest cells becomes structures like the iris, ciliary muscles, choroid, and inner vasculature of the eye. The cornea is derived both from mesenchymal tissue and surface ectoderm.

Disruption of these processes can lead to ocular disease. Microphthalmia, or small eye, and anophthalmia, or no eye, can represent a range of phenotypes, from simple microphthalmia with a small but functional eye to anophthalmia where little or no eye tissue is present (Gujar and Gandhi, 2011). In microphthalmia, the total axial length (TAL) of the ocular orbit is at least two standard deviations below the average. Anophthalmia can be further divided into primary anophthalmia, where the optic vesicles never form; secondary anophthalmia, where the development of the anterior neural tube is disrupted, affecting eye development; and consecutive anophthalmia, where the optic vesicle forms then degrades, leaving some ocular tissue. About 10% of cases of childhood blindness are caused by anophthalmia/microphthalmia (A/M), and most cases of A/M are bilateral. A/M can present with or without a syndrome; approximately one third of cases of A/M are associated with a syndrome (Verma and Fitzpatrick, 2007). Microphthalmia is often present with other eye malformations, including colobomas, which result from failure of the choroid fissure to close. Both genetic and environmental factors can cause A/M. Environmental factors include advanced maternal age (over 40), low gestational age, low birth weight, multiple births, vitamin A deficiency, and congenital infections like rubella, varicella, toxoplasmosis and cytomegalovirus (Gujar and Gandhi, 2011; Verma and Fitzpatrick, 2007). Genetic causes include chromosomal abnormalities like trisomy 18 and mutations in genes like *PAX6*, *SOX2*, *RAX*, *CHX10* and *OTX2*, with *SOX2* being the only major cause of A/M identified, accounting for 10-20 percent of A/M cases (Verma and Fitzpatrick, 2007). Many of the genetic causes of A/M still have yet to be identified, and the aetiology of these deformations is not well understood.

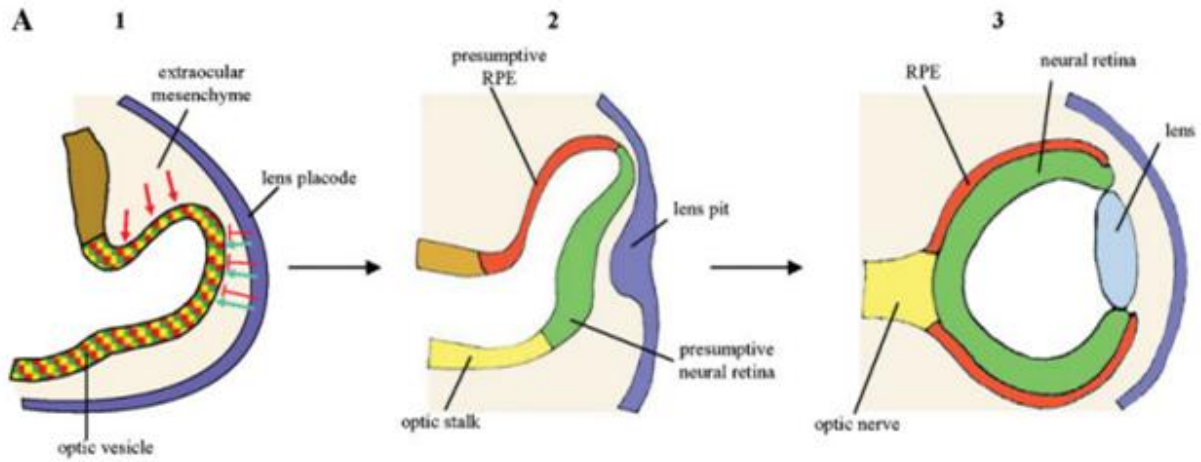


**Figure 7. Formation of the optic cup.** (Martinez-Morales et al, 2004)

Zebrafish is an excellent model for human ocular disease. Eye development in zebrafish occurs very rapidly; the optic vesicle evaginates from the forebrain at 12hpf, and the optic cup forms between 16 and 20hpf (Bibliowicz et al, 2012). The choroid fissure forms at 24hpf and closes by 48hpf. Neurons begin to form at 28hpf and zebrafish can see at around 72hpf. Zebrafish are also similar to humans in their visual information; unlike mice, zebrafish are diurnal, so like humans the majority of visual information is received through cones. Zebrafish contain 4 types of cones: red, green, blue and UV. In humans, diseases that result in retinal degradation may come about by either primary degradation of the retina or primary degradation of the rpe, which in turn causes the retina to degrade without the necessary survival signals and other functions the rpe performs. This degradation then leads to a loss of ocular tissue, loss of vision, and A/M. Zebrafish then are a useful model especially for neural degradation in the eye, as genetic manipulation and study of the affected tissue layers may allow the determination of the root cause of A/M.

Zebrafish mutants with hypopigmentation in the rpe have been described. The zebrafish mutant *silver* with mutations in *pmelb* results in hypopigmentation and increases in undigested POS (Bibliowicz et al, 2012). *pmelb* is important for forming the fibrillar matrix of stage 2 melanosomes in rpe; the interruption of the development of melanosomes affects the recycling of trans-retinal, thereby affecting the photoreceptors. However, how *pmelb* regulates pigmentation in the melanophores of zebrafish is still unknown. More importantly, many other genes regulate pigmentation of melanocytes, and specifically the rpe; determining these genes and their functions will be important in determining genetic causes of rpe and retinal degeneration.

## Transcriptional regulation of pigment cell development

### Paired homeobox family (PAX)

The paired homeobox (*PAX*) family of genes encodes transcription factors containing paired-box DNA-binding domains (Wang et al, 2008). Orthologs of *PAX* genes exist in humans (*PAX*), mice (*Pax*) and zebrafish (*pax*). *PAX* proteins are important during embryogenesis, particularly for maintaining the pluripotency of certain cell-lineages. Two *PAX* proteins, *PAX3* and *PAX6*, are important for the development of neural crest cells and neuroectoderm, respectively.

### PAX3

*PAX3* is located on chromosome 2 in humans (Wang et al, 2008). Expression during development is seen in the central nervous system, in the neural crest and in muscle; mutations in *PAX3* causes Waardenburg syndrome Type 1 (Wang et al, 2008; Read and Newton, 1997). Studies in *Xenopus* have shown that *Pax3* expression is necessary for neural crest cell proliferation and migration, particularly for muscle cells, melanocytes and neurons (Wang et al, 2008). *PAX3* in mammals specifically increases the number of committed melanoblasts early in development, prior to their exit from the neural tube, but also prevents their differentiation. Also important for melanoblast development is the induction by *PAX3* with *SOX10* of *MITF* and *TYRP-1* (Bondurand et al, 2000). The zebrafish orthologs, *pax3a* and *pax3b*, are expressed during development in neural crest and are important for xanthoblast specification (Minchin and Hughes, 2008). In zebrafish, both *pax3a* and *sox10* are necessary for induction of *mitfa* and *tyrp-1* (Elworthy et al, 2003; Murisier et al, 2006). Knockdown using morpholinos of *pax3a* in zebrafish caused a decrease in xanthophore pigmentation and a delayed increase of

melanophores (Minchin and Hughes, 2008). Both orthologs are downregulated once the neural crest cells begin migrating.

### PAX6

In humans, *PAX6* is located on chromosome 11 (Wang et al, 2008). Expression of murine *Pax6* is seen in the CNS, eyes and nose. Humans with heterozygous *PAX6* mutations show aniridia, or lack of iris tissue, and colobomas. Mice heterozygous for mutations in *Pax6* have microphthalmia; homozygous mouse mutations result in failure to develop eye or nasal structures and severe brain abnormalities, and do not survive long after birth. *Pax6* in mice positively regulates rpe development by binding to the promoter of *Mitf* and inducing expression, whereas *Pax2* negatively regulates rpe differentiation (Martinez-Morales et al, 2004). Zebrafish have two orthologs, *pax6a* and *pax6b*; their patterns of expression are distinct but overlapping (Nornes et al, 1998). Both genes are expressed in the developing eye, but *pax6a* is expressed in the medial region of the optic vesicle while *pax6b* is expressed in the lateral regions and in the lens placode. By 24hpf both genes are expressed throughout the optic vesicle. Homozygous mutants for *pax6b* have reduced eye size; the ameliorated phenotype compared to mice is possibly a result of *pax6a* expression (Kleinjan et al, 2008).

### MiT family

The microphthalmia-TFE (MiT) family of proteins are basic helix-loop-helix leucine zipper transcription factors (Hemesath et al, 1994). The MiT family members, MITF, TFEB, TFEC and TFE3, bind DNA sequences as homo- and heterodimers; depending on the transcription factor, this binding can either activate or repress gene expression. Orthologs of these genes exist in many organisms, including humans, mice and zebrafish (Hemesath et al, 1994; Lister et al,

1999). By binding to E box sequences, these proteins regulate cell fate by preventing cell death and promoting survival and differentiation (Hemesath et al, 1994).

### MITF

Microphthalmia-associated transcription factor (*MITF*) is located on chromosome 3 in humans (Tachibana et al, 1994). *Mitf* in mice eyes is induced by Pax6 and Wnt signaling pathways, and along with expression of *Otx1/Otx2* specifies the prospective rpe (Martinez-Morales et al, 2004). Once induced, *Mitf* downregulates expression of *Pax6* and begins to regulate its own expression, and *Pax6* expression becomes restricted to the prospective neural retina. Pax3 induces the expression of *Mitf* in developing neural crest, and leads to the formation of melanoblasts (Wang et al, 2008). Expression of isoforms of *Mitf* is cell type-specific; the M isoform is expressed at high levels in melanocytes, while approximately equal amounts of the A, D and H transcripts are expressed in rpe (Bharti et al, 2012). All these isoforms of MITF bind to M box sequences, an 11 bp sequence that contains an E box sequence, and activate expression of genes related to pigmentation in melanocytes and rpe (Hemesath et al, 1994). These genes include *TYR*, *TYRP1* and *TYRP2*, all of which are involved in melanin production in mammals.

Heterozygous mutations in *Mitf* in mice cause deafness and a white forelock; homozygous mutants show white fur and microphthalmia (Hodgkinson et al, 1993). In humans, heterozygous mutations in *MITF* cause Waardenburg syndrome Type 2A (Read and Newton, 1997). Zebrafish have two orthologs, *mitfa* and *mitfb*; mutations in *mitfa* cause the *nacre* phenotype where fish lose melanophores and gain iridophores (Lister et al, 1999). However, loss of *mitfa* or *mitfb* does not affect the differentiation of the rpe of zebrafish, while the *otx*

family of genes is necessary for the specification of rpe (Lane and Lister, 2012). Disruption of *otx* genes disrupted *mitfa* and *mitfb* expression, but since *mitfa* and *mitfb* knockdowns show normal eye phenotypes, rpe specification is thought to be mediated by another MiT family member.

### TFEC

Transcription factor EC (*TFEC*) is located on chromosome 7 (NCBI) was discovered as a gene with sequence homology with *TFE3* and *TFEB*, especially within the leucine zipper and basic helix-loop-helix domains (Zhao et al, 1993). The researchers found *TFEC* lacked an acidic domain that *TFE3* and *TFEB* contained; this acidic domain gives rise to transactivational activity seen in *TFE3*. *TFEC* binds to E box sequences as homo- or heterodimers like the other MiT family members; however, the effects on transcription are different. While *TFE3* acts to transactivate genes with E3 motifs, *TFEC*-*TFE3* heterodimers inhibit transactivation of these same genes. *Mitf* and *Tfec* are normally expressed in the peripheral retina or presumptive rpe; in *Vsx2* knockouts, failure to repress these genes caused their expression to expand to central retina, leading to an increase in rpe and loss of bipolar cells in the eye (Rowan et al, 2004). Steingrimsson et al (2002) found *Tfec* mutant mice were phenotypically normal and did not alter phenotypes of mice mutant for other MiT family members. No human diseases are associated with mutations in *TFEC*.

In zebrafish, *tfec* expression is observed in the presumptive neural crest and presumptive rpe as early as the 8 somite stage (Lister et al, 2011). Between 16 and 24 hours, *tfec* begins being expressed in the rpe. Around 24 hours expression can be seen on either side of the yolk sac in what will become the lateral patches as well as in the trunk in the dorsal and

ventral stripes, suggesting expression in iridophores. Embryos injected with morpholinos, or morphants, for *tfec* showed a reduction in retinal pigmentation and xanthophores at 48 hours and a reduction in iridophores and xanthophores at 5 days old (unpublished data). The rpe recovered by that timepoint, though it is unclear whether this recovery is due to expression of another gene or the morpholinos being degraded.

#### Interactions of PAX, MITF and TFEC

Knockout mice for *Mitf-D*, the isoform induced by Pax6 and specific to the rpe, showed increased expression of *Tfec* while *Pax6;Mitf* knockouts showed decreased *Tfec* expression, implying *Tfec* is negatively regulated by *Mitf* and positively regulated by *Pax6* (Bharti et al, 2012). However, the Pax6 binding site in the *Tfec* promoter, while conserved among mammals, was not conserved in birds and reptiles. Knockout mice for *Pax6* in rpe showed a decrease in *Tfec* expression; this expression may contribute to the overall phenotype of these mice, as rpe pigment loss is greater in these mice than *Mitf-D* mutants (Raviv et al, 2014). A *Tfec* transgene under a tyrosinase promoter crossed with *Mitf* mutant mice rescued the small-eye phenotype by compensating for the anti-proliferative function of Mitf in the rpe (Bharti et al, 2012). Pax6 alone cannot activate expression of melanogenic genes; however, Pax6 and Mitf, Pax6 and Tfec, and Tfec alone can induce expression of genes like *Tyr* and *Tyrp2* (Raviv et al, 2014). Hemesath et al (1994) found that MITF forms heterodimers with all four other MiT family members, including TFEC.

In neural crest-derived melanocytes Pax3 induces expression of *Mitf-M*; Waardenburg Type 1 and Type 2 cause similar phenotypes even though mutations are in separate loci

because these genes are in the same pathway (Watanabe et al, 1998). *Tfec* is not known to be expressed in any mouse neural crest derivatives (Rehli et al, 2005).

### **Hypothesis and aims**

It was observed that *tfec* expression in zebrafish was increased early in development in the presumptive rpe and presumptive neural crest, tissues which develop into several types of pigment cells. It was also observed that *tfec* morphants have reduced eye pigment and reduced numbers of iridophores and xanthophores. However, the expression of markers of these tissue types has not been established. We hypothesize that with both *tfec* morphants and mutants, the iridophores, xanthophores, melanophores and rpe will be reduced in number and distribution. *In situ* hybridization will be used to demonstrate expression of genes in each of these tissue types. Furthermore, *mitfa* knockout embryos injected with *tfec* morpholinos show a greater pigment deficit. We believe *tfec;mitfa* double mutants will show a more severe phenotype as compared with the morphants.

The rpe phenotype is no longer visible in 4 day old embryos; this recovery of pigment may be due to the morpholino being degraded. We hypothesize that permanent loss-of-function mutations caused by TALENs and CRISPRs will lead to a more severe phenotype in both the developing embryos and adult fish, with losses of rpe, melanophores, xanthophores and iridophores.

## **CHAPTER 2: MATERIALS AND METHODS**

### **Zebrafish culture and maintenance**

Adult fish were maintained at approximately 28°C on a 14 hour/ 10 hour light/dark cycle. Wild type strains (AB/WIK or ZIRC AB) were used for all experiments unless otherwise indicated. Fish homozygous for the *mitfa*<sup>w2</sup> allele were generated as described by Lister et al (1999). Embryos were incubated at 28°C and staged according to Kimmel et al (1995).

### **Generating *tfec* mutations**

Sander et al (2011) described the use of designed TAL effectors to target FokI nucleases to sequences of interest in zebrafish. The TALENs for exon 8 of *tfec* were designed using the Cornell University TAL Effector Targeter 2.0 and constructed using the Golden Gate 2.0 TALEN Assembly Kit from Daniel Voytas and Adam Bogdanove (Addgene: 1000000024) as described in Cermak et al (2011). The TALENs for exon 3 were designed and constructed by the Joung lab at Massachusetts General Hospital and obtained from Addgene (plasmids 41368 and 41369). The primers used and expected product sizes are listed in Table 1.

TALENs for both exon 3 and exon 8 targeted near an MboI restriction enzyme site. Successful double-strand breaks with non-homologous end joining that resulted in insertions or deletions would disrupt MboI digestion following PCR amplification.

### Screening potential founder fish

To identify germline carriers of the *tfec* mutation, intercrosses were set up and embryos were collected from these matings. Embryos aged at 72 hpf were pooled in groups of four in tubes to facilitate faster identification of carriers. ZIRC lysis buffer (50  $\mu$ l) [1.5 mM MgCl<sub>2</sub>, 10 mM Tris-HCl (pH = 8.3), 50 mM KCl, 0.3% Tween-20 (20%), 0.3% NP-40 (20%) in water] was added to each tube and DNA was prepared by heating the samples in heat blocks through the following steps: 10 minutes at 95°C, followed by addition of 5 $\mu$ l Proteinase K (10 mg/ml) and incubation at 55°C for one hour, and a final incubation at 95°C for 10 minutes to inactivate the Proteinase K. The tubes were then vortexed and spun in a nanofuge.

### PCR

The GoTaq Green Master Mix (Promega) was used for the reaction (Table 1). The samples were heated to 94°C for 4 minutes, 94°C for 30 seconds, 62°C for 30 seconds, 72°C for 30 seconds, and steps 2-4 were repeated for 39 cycles. The samples were then incubated at 72°C for 10 minutes then held at 4°C.

The amplified product was digested at 37°C with Mbol (New England Biolabs, NEB) for at least 1 hour. Then, 2  $\mu$ l of 6X loading dye was added and 6  $\mu$ l of the digested product was run on a 3% high-resolution agarose gel. All gel pictures were taken using the AlphaImager software. Heterozygous samples were identified by the presence of an undigested band at ~323 base pairs (Table 2). Digests were repeated of samples with undigested bands, 2  $\mu$ l of 6X loading dye was added and 10  $\mu$ l of the digested product was run on a 3% high-resolution agarose gel. Undigested bands were excised prior to photographing using AlphaImager

software. DNA was extracted from this band using the Bioline ISOLATE II PCR and Gel Kit and eluted into 15 µl Elution Buffer (Bioline).

Primer names	Sequences
w2-for	tgtggattgaggttccttc
w2-rev	ttgcatgtgctgattgttca
tfec-ex3F	GACGCGTCTGTTATTGGATTAGCG
tfec-ex3R	GCCACAGCACATAACAACAGGTC
C3	CCGCTGGTGCTCCTCCTT
Cex8TAL-F	ttgctgtgaggagacagtgc
cex7F	aggcaaggtaatgtccgaga
cex7R	TGGATCCGTAGCTGGAGTCT

**Table 1. Primer sequences used in this study.**

Primer Pair	Enzyme	Wild-type bands (bp)	Mutant band(s) (bp)
tfec-ex3F/tfec-ex3R	Mbol	189 & 134	~323
C3/Cex8TAL-F	Mbol/AlwNI	310, 91, & 49	~360 & 91
w2-for/w2-rev	Dral	192 & 123	123, 98 & 94
cex7F/cex7R	StuI	208 & 102	~310

**Table 2. Expected product sizes of PCR and subsequent digestion where applicable.**

*TOPO Cloning (Invitrogen protocol) and Transformation*

The purified product was then cloned into the pCR4-TOPO vector. Clones were additionally screened by digestion with DpaI; 2 µl of 6X loading dye were added to each tube, and 6 µl of the digest were run on a 1% agarose gel. Clones with a band at about 1,400 base pairs were sequenced in the VCU Nucleic Acids Research Facilities to identify the mutation produced by the TALENs. Intercrosses yielding embryos with sequenced mutations were repeated, and the resulting embryos were raised to adulthood.

### Fin clipping for genotyping

To identify mutation carriers, DNA was prepared from fin clip biopsies and genotyped using PCR and restriction digestion with the appropriate enzymes. Adult fish were anaesthetized in ethyl 3-aminobenzoate, methanesulfonic acid salt 98% (MESAB) (Acros). A triangular portion of the caudal or tail fin about 5 mm on each side was clipped off using a sterilized razor blade. Using sterilized forceps, this fin biopsy was placed in ZIRC lysis buffer (50  $\mu$ l). DNA was prepared by heating the samples in heat blocks through the following steps: 10 minutes at 95°C, followed by addition of 5 $\mu$ l Proteinase K (10 mg/ ml) and incubation at 55°C for one hour, then a final incubation at 95°C for 10 minutes to inactivate the Proteinase K. The tubes were then vortexed and spun in a nanofuge and 1:50 dilutions of the DNA were made in nuclease-free water to be used for genotyping. PCR reactions were carried out identically to those described above.

### **Genotyping the *mitfa*<sup>w2</sup>;*tfec* double mutants**

Individual embryos at 72 hpf were photographed using a SZX12 dissecting stereomicroscope with DP70 camera (Olympus) then placed in tubes. ZIRC lysis buffer (50  $\mu$ l) was added to each tube. DNA was prepared by heating the samples in heat blocks through the following steps: 10 minutes at 95°C, followed by addition of 5 $\mu$ l Proteinase K (10 mg/ ml) and incubation at 55°C for one hour, then a final incubation at 95°C for 10 minutes to inactivate the Proteinase K. The tubes were then vortexed and spun in a nanofuge.

Two separate sets of PCR reactions were used to genotype the *tfec* allele and the *mitfa*<sup>w2</sup> allele (Table 1). The GoTaq Green Master Mix (Promega) was used for the reaction. The samples were heated to 94°C for 4 minutes, 94°C for 30 seconds, 62°C for 30 seconds, 72°C for

30 seconds, and steps 2-4 were repeated for 39 cycles. The samples were then incubated at 72°C for 10 minutes then held at 4°C.

The amplified *tfec* product was digested at 37°C with MboI (New England Biolabs, NEB) for at least 1 hour; *mitfa*<sup>w2</sup> alleles were treated with DraI (NEB) for at least one hour (Table 2). Then, 2 µl of 6X loading dye was added and 6 µl of the digested product was run on a 3% high-resolution agarose gel. All gel pictures were taken using the Alphamager software.

### **Morpholino injections**

Two splice-site blocking morpholino oligonucleotides against *tfec* were obtained from Gene Tools (Philomath, OR). The portions of the sequences complementary to the splice site donor GT are underlined.

*tfec* E515: 5' AGCCTAAAAACCACTTACTTAGATT 3'

*tfec* E616: 5' CTTGTCAGATTTCAACTTACGGGTC 3'

Morpholinos were co-injected at a total concentration of 2.5 ng/ embryo, 1.25 ng each morpholino. Larvae examined for morphological changes were anesthetized in MESAB and eye and pigmentation were examined using a SZX12 dissecting stereomicroscope with DP70 camera (Olympus).

### **CRISPR/Cas9 injections**

The CRISPR for exon 7 of *tfec* was designed using the CHOPCHOP web tool and was constructed using the protocol described in Talbot and Amacher (2014). CRISPR guideRNA diluted to 100 ng/µl was coinjected with Cas9 at a concentration of 100 ng/µl. Larvae examined for morphological changes were anesthetized in MESAB and eyes and pigmentation were examined using a SZX12 dissecting stereomicroscope with DP70 camera. Eye sizes were

measured using the elliptical tool on ImageJ software. Area in pixels was used to estimate relative sizes of the eyes of both controls and CRISPR-injected embryos. Embryos were genotyped using GoTaq Green Master Mix (Table 1). The samples were heated to 94°C for 4 minutes, 94°C for 30 seconds, 62°C for 30 seconds, 72°C for 30 seconds, and steps 2-4 were repeated for 39 cycles. The samples were then incubated at 72°C for 10 minutes then held at 4°C. PCR amplification was followed by digestion with *StuI* overnight at 37°C (Table 2). Undigested bands following gel electrophoresis were excised and cloned into pCR4-TOPO vectors and sent for sequencing. Gels were photographed using AlphaMager software.

### ***In situ* hybridization (ISH)**

For analysis of expression beyond 24 h of development, embryos were incubated with 0.003% 1-phenyl-2-thiourea (PTU) to inhibit melanin synthesis prior to fixation. Dechoriation was done manually and embryos were fixed for 24 hours in 4% paraformaldehyde (PFA) in 1X phosphate buffered saline (PBS) (USB Corporation). A quick rinse in PBS + 0.05% Tween-20 (PBT) was then followed by overnight dehydration in methanol (MeOH). Embryos were rehydrated in a MeOH/ PBT series (66% MeOH/33% 1X PBT; 33% MeOH/66% 1X PBT; 1X PBT) for 5 minutes each with 4 repeats of the final PBT wash. Embryos older than 24 hours were digested in Proteinase K (1 µg/ml in 1XPBT) for one minute per hour of age (ie 48hpf=48 minutes) then post-fixed in 10% formalin for 20 minutes. Following the post-fix was four washes of 1X PBT for 5 minutes per wash.

Embryos were prehybridized for at least 1 hour in hybridization buffer [50 % formamide, 5X Sodium citrate buffer (SSC) (USB Corporation), 50 µg/ml heparin, 0.5 mg/ml tRNA, 0.1%

Tween-20, 9.2 mM Citric acid, nuclease-free water] (Hyb+) at 65°C. Embryos were incubated overnight at 65°C with the diluted probes. Washes at 65°C followed hybridization: quick wash in hybridization buffer without heparin and tRNA (Hyb-), 15 minute wash in 66% Hyb-/33% 2XSSC, 15 minute wash in 33% Hyb-/66% 2XSSC, 15 minute wash in 2X SSC, and two 20-minute washes in 0.2X SSC. Washes at room temperature followed (66% 0.2X SSC/ 33% 1X PBT; 33% 0.2X SSC/ 66% 1X PBT; 1X PBT) for 5 minutes in each solution.

Embryos were then incubated in blocking solution [2mg/ml bovine serum albumin (BSA) and 2% goat serum in 1X PBT] for at least 1 hour, followed by overnight labelling at 4°C in alkaline-phosphatase-coupled antidigoxigenin Fab fragments (Roche) at 1:10,000 dilution in blocking solution. The embryos were then quick-washed in 1X PBT, washed 5 times in 1X PBT for 10 minutes each at RT followed by three 5-minute washes in coloration buffer [0.1 M Tris hydrochloride (pH 9.5), 50 mM MgCl<sub>2</sub>, 0.1 M NaCl, .1% Tween-20].

Finally, the coloration reaction was performed in the dark using nitro blue tetrazolium 24 chloride (NBT) [225µg/ ml] and 5-bromo-4-chloro- 3'-indoly]phosphate p-toluidine salt (BCIP) [175 µg/ ml] in coloration buffer. The reaction was halted with a quick wash of 1X PBT after color had developed, and the embryos were dehydrated in MeOH for 30 minutes to clear out background. The embryos were then rehydrated through the MeOH/ PBT series and equilibrated in 50% glycerol in 1X PBT for viewing and photographing. Pictures of embryos were taken with the Olympus SZX12 confocal microscope using the DP Controller software. Previously validated probes were used to detect expression of *dct* (Kelsh et al., 2000), *fms* (Parichy et al., 2000), *xdh* (Parichy et al, 2000), *ltk* (Lopes et al., 2008) and *pmelb* (Schonthaler et al., 2005).

## **CHAPTER 3: RESULTS**

### **Sequencing of TALEN-derived and CRISPR-derived mutants**

The mutation in *mitfa* causes loss of neural-crest derived melanosomes, reduction in xanthophore pigmentation, and an increase in iridophores (Lister et al, 1999). However, previous experiments have shown that *mitfa* mutations do not affect rpe development of embryos (Lane and Lister, 2012). Furthermore, injection of *tfec* morpholinos in both wild-type and *mitfa* mutant embryos resulted in reduced eye melanin, xanthophore and iridophore pigments; the reduced eye pigmentation recovered by day 4, making it difficult to determine if this recovery was due to the morpholinos being degraded or compensation by another gene.

Transcription activator-like effector nucleases (TALENs) are composed of TAL effector repeat domains bound to a DNA cleavage domain (Boch and Bonas, 2009; Moscou and Bogdanove, 2009). The repeat domains contain variable regions that have different specificities for different base pairs of DNA; these repeat domains can then be designed to bind specific regions of DNA, where the nuclease cleaves and induces double stranded breaks (DSB). The cell repairs these breaks via non-homologous end-joining (NHEJ), which is an error prone process and sometimes results in insertions and/or deletions. Because of the binding specificity and the induction of permanent heritable mutations, coupled with the ability to inject zebrafish embryos at the one cell stage, TALENs are useful in creating lines of mutant zebrafish.

Therefore, TALENs were designed to target two exons in *tfec*: exon 8, which codes for a leucine zipper (Figure 8), and exon 3, which codes for the activation domain (AD) (Figure 10) (Lister et al, 2011).

The CRISPR/Cas9 system was also used to generate mutants. The clusters of regularly interspaced short palindromic repeats (CRISPR) defense system in bacteria uses viral DNA as a guide to bind and degrade DNA using CRISPR-associated (Cas) proteins (Brouns et al, 2008). Researchers have been able to successfully induce mutations by designing a guide RNA (gRNA) to zebrafish genes and coinjecting the designed CRISPR with Cas proteins (Jao et al, 2013). One target gRNA of about 20 base pairs is required for gene-specific targeting, making CRISPR/Cas9 assembly simpler than TALENs (Schulte-Merker and Stainier, 2014). Furthermore, injection of CRISPR/Cas9 systems can result in homozygous mutations when injected at high enough concentrations, resulting in a visible phenotype without having to cross fish and raise subsequent generations (Jao et al, 2013; Schulte-Merker and Stainier, 2014). Therefore, one CRISPR gRNA was designed to target exon 7 in *tfec*, coding for the second helix in the helix-loop-helix domain (Figure 12) (Lister et al, 2011).

### Exon 8

High resolution melting assay (HRMA) was used to identify potentially mutated samples. These identified samples were used in PCR reactions and were subsequently digested with Mbol. Sequencing of embryo pools with lowered DNA melting points showed 3 base pair deletions that were in frame. One resulted in the loss of a leucine while the other lost an isoleucine and glutamine, creating a new codon for methionine (Figure 9). The F1 fish were screened using fin clip biopsies to identify carriers, which were crossed to yield F2 embryos.

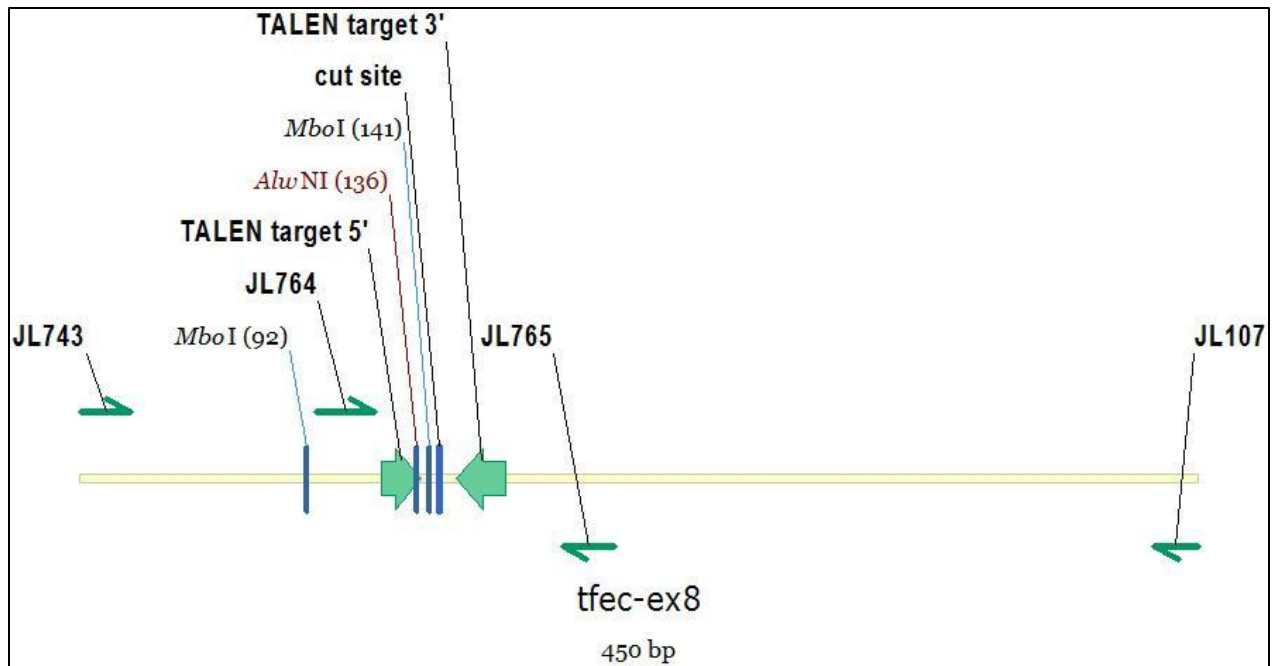


**Figure 8. Diagram of exon 8 of *tfec*.** TALEN target sites are shown. Primers 764 and 765 were used for most of the genotyping of the mutant alleles. Digestion of MboI was used as the site lay between the two TALEN targets adjacent to the predicted cut site.

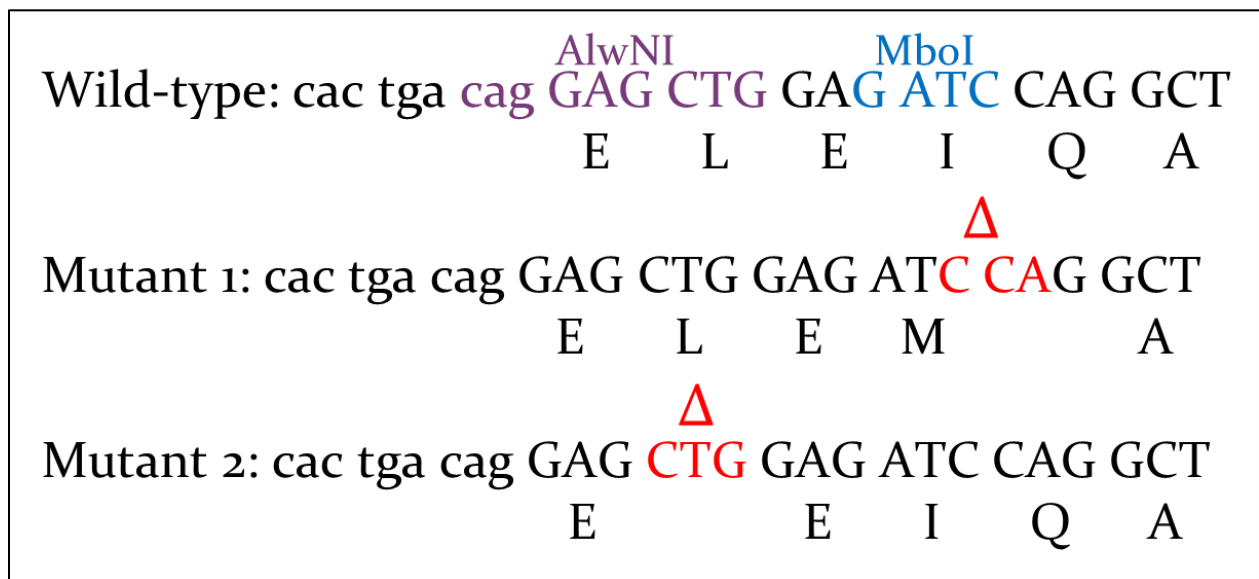


**Figure 9. Sequences of mutants in exon 8 of *tfec*.** All sequences read 5' to 3'. The top sequence shows two enzymes, AlwNI and MboI used in genotyping mutants. Both lines of fish showed a 3 base pair deletion, one between 2 codons resulting in a methionine, the other of a leucine within the leucine zipper.

Exon 3

Germline carriers were identified using PCR and restriction digest and were used to establish a stable mutant line. Sequencing of undigested bands yielded two variants: an in-frame 3 base pair deletion of a leucine and a 4 base pair deletion that caused an early stop codon (Figure 11). Germline carriers were intercrossed to generate F1 carriers with wild-type background as well as outcrossed to yield carriers of mutations in *tfec* and *mitfa*. The F1 fish were screened using fin biopsies to identify carriers and were crossed to yield F2 embryos.

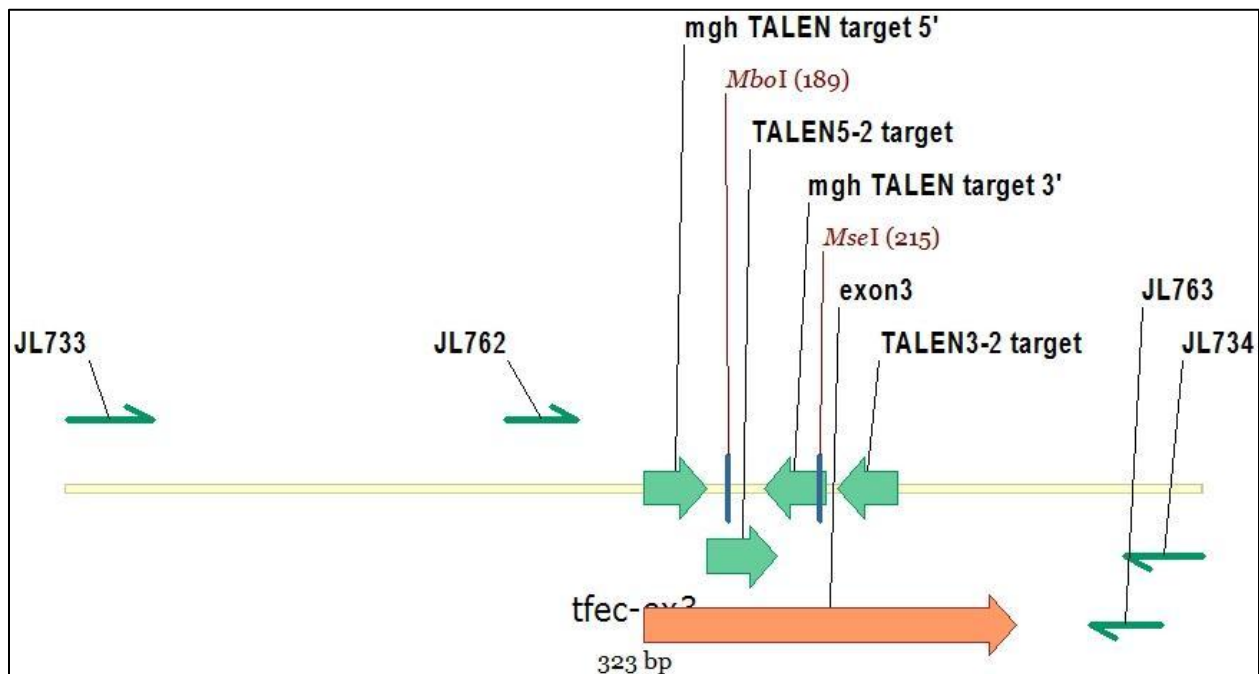


**Figure 10. Diagram of exon 3 of *tfec*.** Primers 733 and 734 were used for most of the genotyping of the mutant alleles. The mgh TALEN targets were used to create the line of fish used in the described experiments. Digestion of MboI was used as the site lay between the two TALEN targets adjacent to the predicted cut site.

Wild type:

5'-GAC <sup>MboI</sup> GAT CTT ATT GGC CTT GAA-3'  
D E L I G L E

Mutant 1:

5'-GAC <sup>Δ</sup> GAT CTT ATT GGC CTT GAA-3'  
D L I G L E

Mutant 2:

5'-GAC <sup>Δ</sup> GAT C TTA TTG GCC TTG AAA ACG GTT TTA  
D L L A L K T V L  
AGG ATG GGA GCT TGG ATT GCA TGG AGC CAG  
R M G A W I A W S Q  
GCA TCA TAA-3'  
A S stop

**Figure 11. Sequencing results of TALEN-derived *tfec* exon 3 mutants.** The top sequence represents the wild-type sequence of the *tfec* allele, which has an MboI site (in blue). The first mutant found had a 3 base pair, in-frame deletion resulting in the loss of a single glutamate (in red). The second mutant found had a 4 base pair deletion (red) that resulted in an early stop codon.

## Exon 7

Injected embryos were photographed at several timepoints then sorted into individual tubes for genotyping with PCR analysis and subsequent restriction enzyme digestion. Sequencing of several undigested bands revealed several mutations (Figure 13). Of the four sequenced embryos, two showed 6 base pair, in-frame deletions, one showed a 21 base pair, in-frame deletion, and another showed a 10 base pair deletion with no early stop codon.

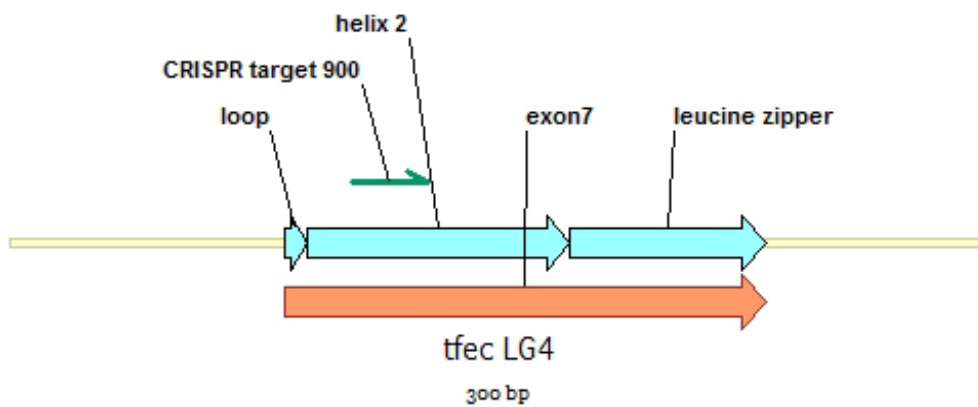


**Figure 12. Diagram of the binding site for the CRISPR guideRNA for exon 7.**

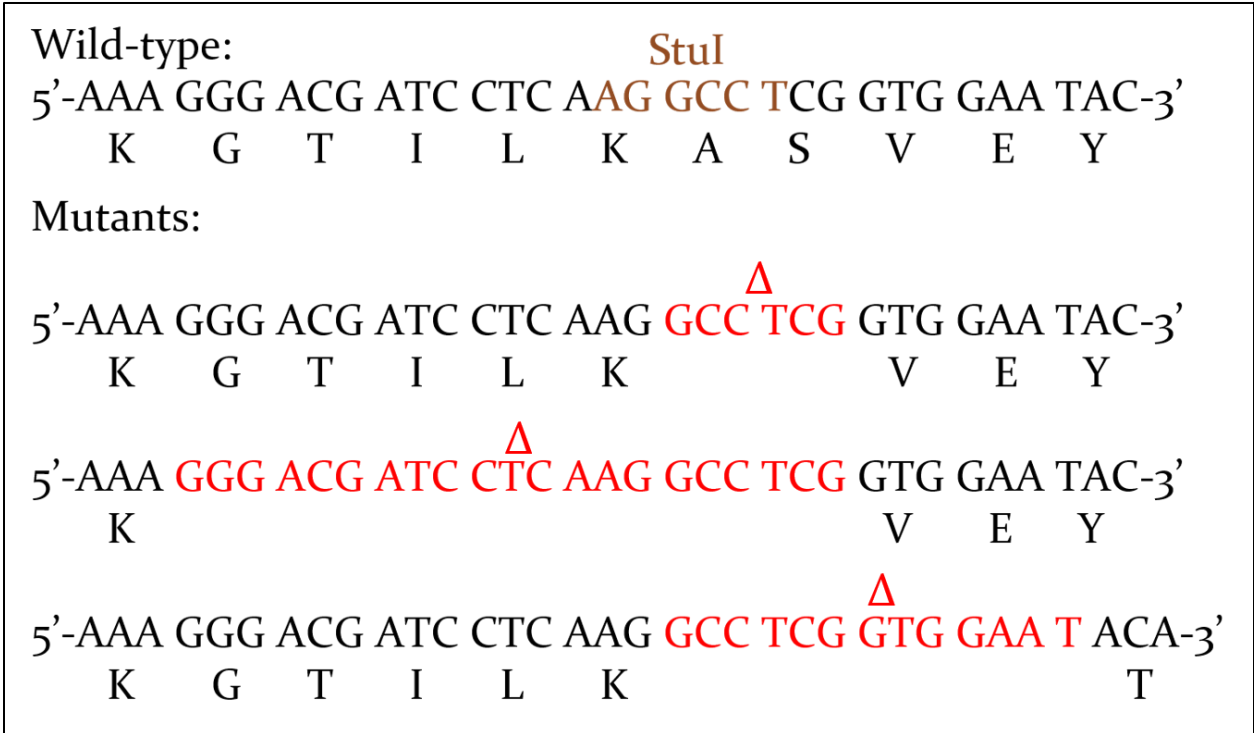


**Figure 13. Sequences of several *tfec* exon 7 mutants.** The top sequence shows the wild-type sequence with the StuI site shown in orange. The first mutant has a six base pair in-frame deletion (deletions in red). The exact base pairs deleted are ambiguous; one possible deletion is shown. The second has a 21 base pair in-frame deletion, while the third is a 10 base pair deletion with no early stop codon.

## ***tfec* morphants and mutants show delayed pigmentation and *rpe* development**

*In situ* hybridizations with probes against *tfec* revealed expression in the presumptive *rpe* and presumptive neural crest as early as the 8 somite stage (Lister et al, 2011). Previous data using morpholinos against *tfec* showed losses of melanophores in the eye, xanthophores and iridophores. However, there are several drawbacks with using morpholinos alone to determine a phenotype. One drawback is that the effects of the morpholino are short-lived; the translation of the mRNA into protein is suppressed for about two days, which prevents long-term study of a gene's activity throughout development (Nasevicius and Ekker, 2000). Another is that non-specific effects of morpholinos make determining the phenotype from the gene of interest difficult and sometimes inaccurate (Schulte-Merker and Stainier, 2014). Kok et al (2015) found that 80 percent of published morphant phenotypes described as part of the Sanger Zebrafish Mutation Project were not seen in mutant embryos. Therefore, use of genome editing technologies that create permanent mutations in the genome in the injected generation is of interest to corroborate results seen with morpholinos.

In these experiments, morpholinos and CRISPRs were used to generate morphants and mutants respectively of *tfec* and to corroborate the findings. Embryos injected with CRISPR/Cas9 directed against exon 7 of *tfec*, which codes the second helix of the helix-loop-helix domain, were raised for several days and photographed at the following timepoints: 48hpf, 72hpf, 96hpf, and 120hpf. Both morpholino- and CRISPR/Cas9-injected embryos were fixed at several timepoints (24hpf, 48hpf and 72hpf) and *in situ* hybridizations were used to evaluate changes in expression of markers of various tissue types (Table 3).

Probe	Background	Control/MO/CRISPR	Timepoint (hpf)	Normal marker	Reduced/absent marker	Total	
<i>dct</i>	AB/WIK	Control	24	20	1	21	
		MO	24	2	20	22	
		Control	48	22	1	23	
		MO	48	5	19	24	
		Control	72	23	0	23	
		MO	72	19	3	22	
	<i>mitfa</i> mutant	Control	24	18	0	18	
		MO	24	4	19	23	
		Control	48	18	1	19	
		MO	48	5	14	19	
		Control	72	19	0	19	
		MO	72	3	18	21	
	<i>pmelb</i>	AB/WIK	Control	24	21	1	22
			CRISPR	24	2	17	19
Control			48	24	0	24	
CRISPR			48	2	19	21	
Control			72	26	3	29	
CRISPR			72	20	5	25	
<i>mitfa</i> mutant		Control	24	22	0	22	
		CRISPR	24	4	35	39	
		Control	48	21	3	24	
		CRISPR	48	1	21	22	
		Control	72	27	2	29	
		CRISPR	72	1	17	18	
<i>xdh</i>	AB/WIK	Control	24	21	0	21	
		MO	24	0	23	23	
		Control	48	15	5	20	
		MO	48	0	25	25	
		Control	72	18	6	24	
		CRISPR	72	2	15	17	
	<i>mitfa</i> mutant	Control	24	0	25	25	
		MO	24	4	17	21	
		Control	48	25	1	26	
		MO	48	2	21	23	
		Control	72	11	3	14	
		MO	72	0	15	15	

<i>fms</i>		Control	24	20	0	20
		MO	24	13	7	20
	AB/WIK	Control	48	13	8	21
		MO	48	0	22	22
		Control	72	34	1	35
		CRISPR	72	0	14	14
	<i>mitfa</i> mutant	Control	24	17	3	20
		CRISPR	24	5	18	23
		Control	48	29	0	29
		CRISPR	48	2	22	24
		Control	72	31	1	32
		CRISPR	72	18	0	18
<i>ltk</i>		Control	24	10	5	15
		CRISPR	24	2	18	20
	AB/WIK	Control	48	28	2	30
		CRISPR	48	3	11	14
		Control	72	23	0	23
		CRISPR	72	0	17	17
	<i>mitfa</i> mutant	Control	24	30	0	30
		MO	24	23	6	29
		Control	48	19	0	19
		CRISPR	48	5	12	17
		Control	72	35	0	35
		CRISPR	72	2	27	29

**Table 3. Number of *in situ* hybridizations for each marker, background and timepoint.**

### *tfec mutants and morphants show delayed eye melanogenesis*

Melanogenesis begins at 24hpf, but pigmentation is not visible until 28hpf, when dorsal melanophores become visible from the head through the yolk sac, and the rpe darkens (Kimmel et al, 1995). Melanophores continue to differentiate rostrocaudally; at 42hpf, melanophores are present from head to tail, and the dorsal and ventral stripes are present but disorganized. The lateral and yolk stripes develop after 48hpf.

Previous data had shown reduced eye pigmentation in *tfec* morphants. At 48hpf and 72hpf, mutant embryos show a reduction in melanin pigment, especially in the medial portion of the eye (Figure 14). The loss of pigment at the back of the eye creates the appearance of a ring of pigment, rather than the more homogeneous pigmentation seen in the wild-type embryos. By 96hpf, most of the eye pigment recovers, with the exception of what appears to be colobomas within the iris. The absence of melanophores within the lateral patches is visible. Eye pigmentation is fully recovered by 120hpf, suggesting mutations in *tfec* merely cause a delay in melanogenesis in the eye. Melanophores are also present by this point in the lateral patches.

Embryos injected with morpholinos show a reduction in expression of dopachrome tautomerase (*dct*), which is induced in zebrafish by *mitfa* (Johnson et al, 2011). *dct* or *tyrp2* is expressed in melanin-producing cells because this enzyme converts dopaquinone to eumelanin. Therefore, *dct* expression is used as a marker for melanoblasts. At 24hpf, there is no *dct* expression in morphant zebrafish, and at 48hpf and 72hpf, *dct* expression in the eye is less than in wild-type embryos (Figure 15). The *in situ* expression data correlates with the morphological data that *tfec* knockdown and knockout causes a delay in melanogenesis by the rpe.

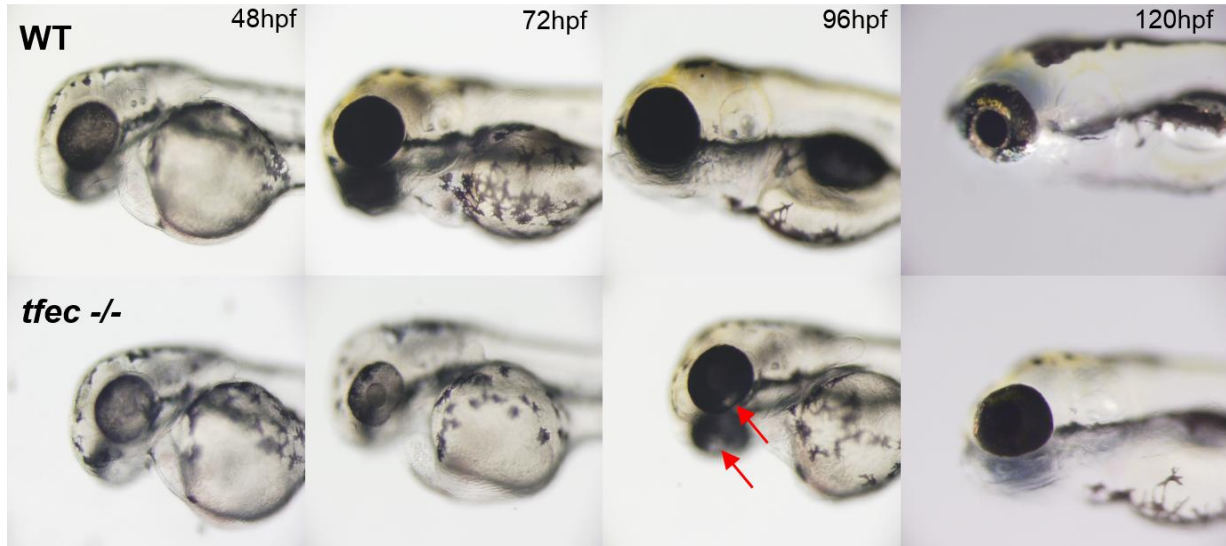


**Figure 14. Delayed eye melanogenesis and growth in *tfec* mutants.** Eye melanogenesis is reduced at 48 and 72hpf, and eye size is smaller in injected embryos at 72hpf. The greatest loss of pigmentation is in the medial retina. By 96hpf, eye melanogenesis has returned to normal levels, and eye size matches that of controls by 120hpf. Injected embryos also show colobomas at 96hpf (red arrows), though these have closed by 120hpf. 48, 72 and 96hpf photographs taken with transmitted light; 120hpf taken with incident light.

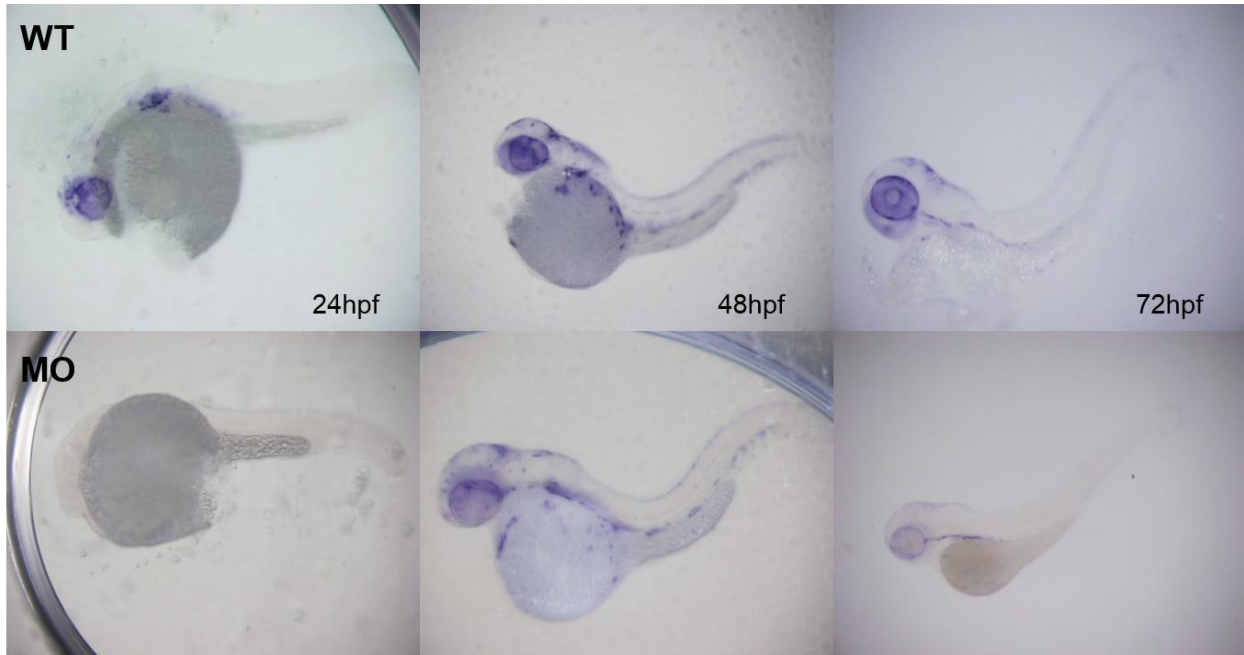


**Figure 15. Morphant embryos for *tfec* show a delayed expression of *dct*.** 24hpf embryos show no expression. 48hpf and 72hpf show reduced expression, especially in the eye.

*tfec* mutants show reduced expression of markers for rpe

Premelanosome protein b (*pmelb* or *silvb*) is expressed in melanoblasts, specifically within the melanosomes of the rpe, and helps give structural organization to the early stage organelles; in mice, knockout of *Pmel* causes silver hair pigment and circular, immature melanosomes in the choroid and retina (Hellstrom et al, 2011). Zebrafish have two orthologs, *pmela* and *pmelb*; while *pmela* is expressed in both melanophores and rpe, *pmelb* expression is limited to the rpe (Schonthaler et al, 2005). *pmelb* expression is then used to visualize the developing rpe in zebrafish. At 24hpf and 48hpf, embryos injected with CRISPR/Cas9 showed a greater loss of *pmelb* expression compared to wild-type embryos, with the greatest amount of expression lost in the medial and ventral portions of the eye (Figure 16). By 72hpf, most of the expression of *pmelb* is recovered, so the marker for rpe is merely delayed.

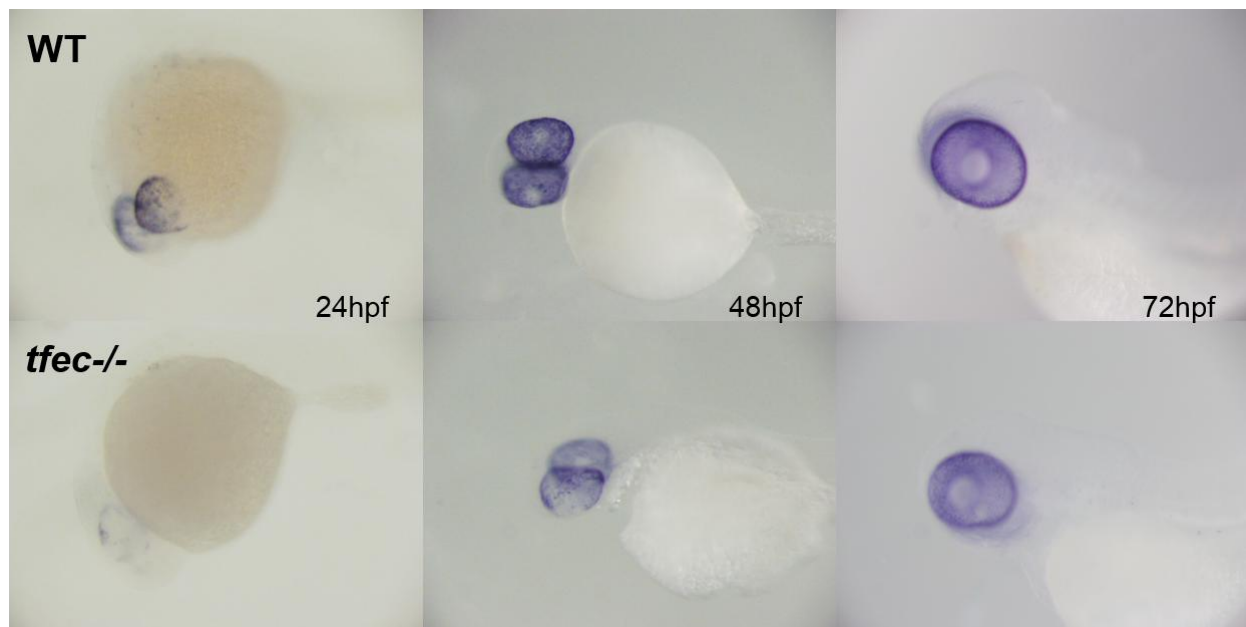


**Figure 16. Delayed expression of *pmelb* in eyes of *tfec* mutant embryos.** 24hpf embryos show little expression of *pmelb* except for in the peripheral retina. Expression of *pmelb* is reduced in 48hpf embryos, with less expression in the medial and ventral retina. By 72hpf, expression resembles that of wild-type embryos.

### *tfec mutants have reduced eye size*

Disruption of genes regulating eye development can affect eye size and shape; for example, in humans, mutations in *SOX2* cause A/M in 10-20 percent of cases (Verma and Fitzpatrick, 2007). In zebrafish, several genes and environmental factors have been described that cause microphthalmia or anophthalmia in zebrafish when mutated or disrupted. Many mutations causing eye abnormalities affect the rpe, specifically the degradatory function of the melanosomes (Bibliowicz et al, 2012). For example, knockdown of *pmelb* results in zebrafish with defective rpe and microphthalmia.

Because the *tfec* morpholino injections caused a delay in melanogenesis, specifically in the rpe as evidenced by the *dct* and *silvb* expression data, eye size was also examined. At 48hpf, the embryos eye sizes were the same (Figure 14). By 72hpf the eyes were smaller in the injected embryos than in the controls, and this continued to 96hpf. Once the embryos reached 120hpf the eyes were comparably sized to the control embryos. Furthermore, the overall head size of the injected embryos seems to also be smaller, following the same trend of size as the eyes, though at 120hpf the heads were smaller than the wild-type embryos. Eye sizes were measured using ImageJ software, and were plotted on a line graph showing changes in area over time (Figure 17). Further measurements are needed for statistical significance.

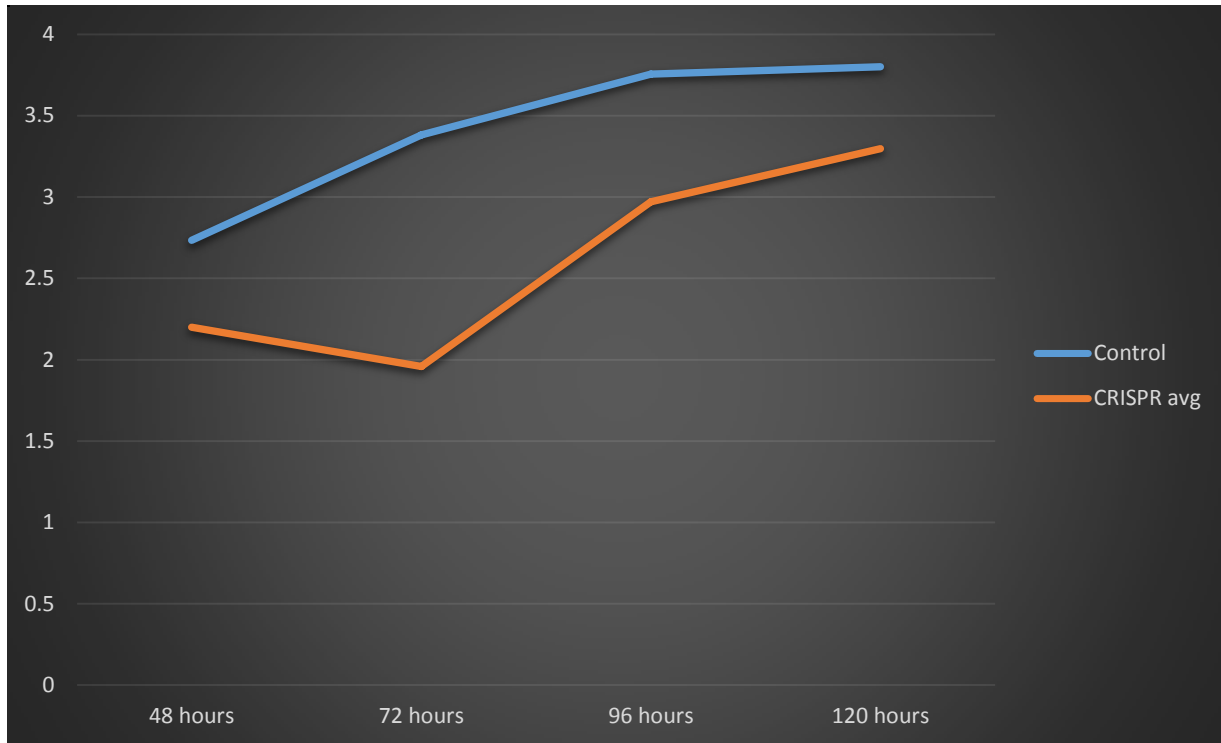


**Figure 17. Eye areas of control and CRISPR-injected embryos.** Eye areas were measured using ImageJ software, and were plotted as pixels at each timepoint in order to show relative sizes. Photographs were taken at the same magnification. At 48 and 120hpf, eye sizes were similar, while at 72hpf and 96hpf eyes were smaller. More measurements are needed to ascertain significance.

### *tfec mutants and morphants show delayed xanthophore pigmentation*

Wild-type embryos show xanthophore pigmentation by 72hpf, visible as a yellow hue through the body of the embryo, developing first in the head around 42hpf then continuing rostrocaudally until the trunk has the same hue (Kimmel et al, 1995). Previous experiments with *tfec* morphants showed a reduction in xanthophore pigmentation in wild-type embryos. No yellow pigmentation is visible in the head of the injected embryos at 48hpf (Figure 18). At 72hpf, wild-type embryos have developed xanthophore pigmentation while the CRISPR-injected embryos have not. Pteridine pigment is still not visible in mutant embryos by 96hpf; however by 120hpf, xanthophore pigmentation is visible but reduced in the head and trunk.

Two probes, *xdh* and *fms*, were used to evaluate the expression of genes related to xanthophore pigmentation. Xanthine dehydrogenase (*xdh*) synthesizes the xanthophore pigment xanthopterin from pteridine, and therefore is expressed in xanthoblasts throughout development, while colony stimulating factor 1 receptor a (*csf1ra* or *fms*) is required for xanthoblasts to migrate correctly and separate from the neural crest (Parichy et al, 2000). Therefore, expression of both of these markers can be used to study the development of xanthophores. At 24hpf, expression of *xdh* is absent in the injected embryos, and is still absent at 48hpf (Figure 19). By 72hpf, some expression is present in the head, but is less than the wild-type embryos. Expression of *fms* is present but lesser at 24hpf when compared to time-matched controls, and is absent from 48hpf embryos (Figure 20). As with the *xdh* probe, by 72hpf expression of *fms* is present in the head but is less than in controls. Knockdown and

knockout of *tfec* causes a delay in xanthophore pigmentation, seen in the morphology of the embryo and the *in situ* hybridizations.

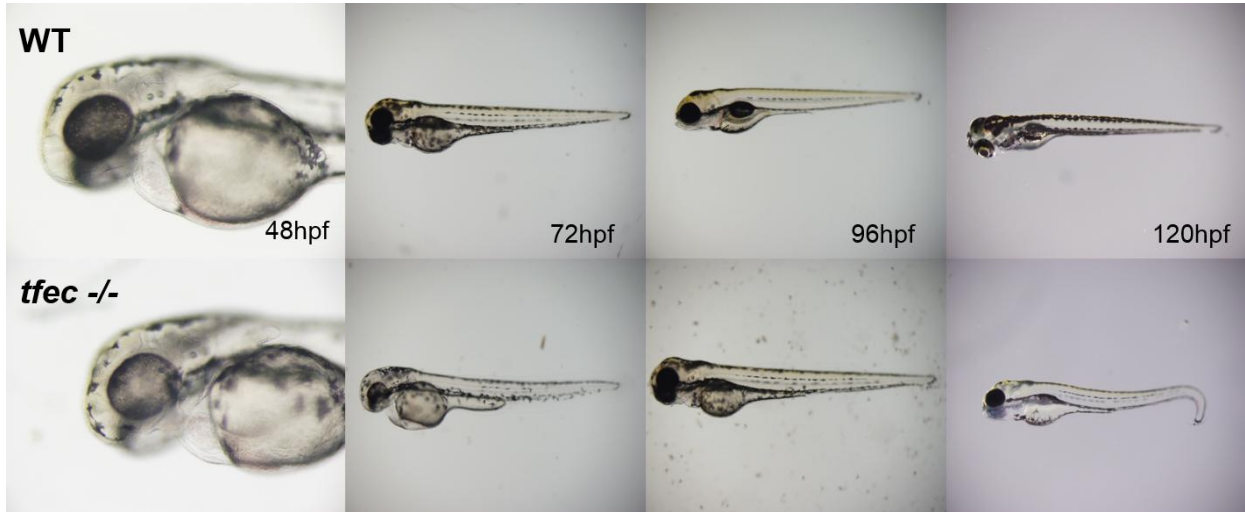


**Figure 18. Xanthophore pigmentation is delayed in *tfec* mutants.** Xanthophores are absent from the heads of CRISPR-injected embryos at 48hpf, and the heads and trunks of embryos at 72hpf. At 96hpf and 120hpf, xanthophore pigmentation is visible.

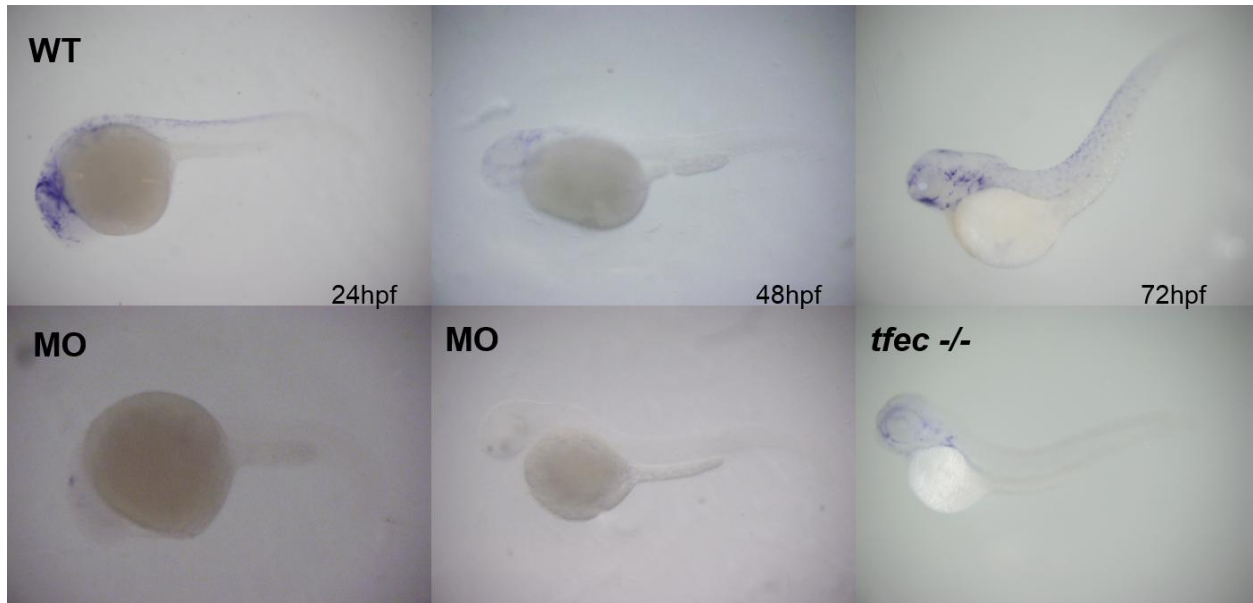


**Figure 19. Morphant embryos for *tfec* show loss of expression of *xdh*.** Morphant embryos show no expression of *xdh* at 24hpf or 48hpf. At 72hpf, limited expression is seen in the head and no expression is seen in the trunk.

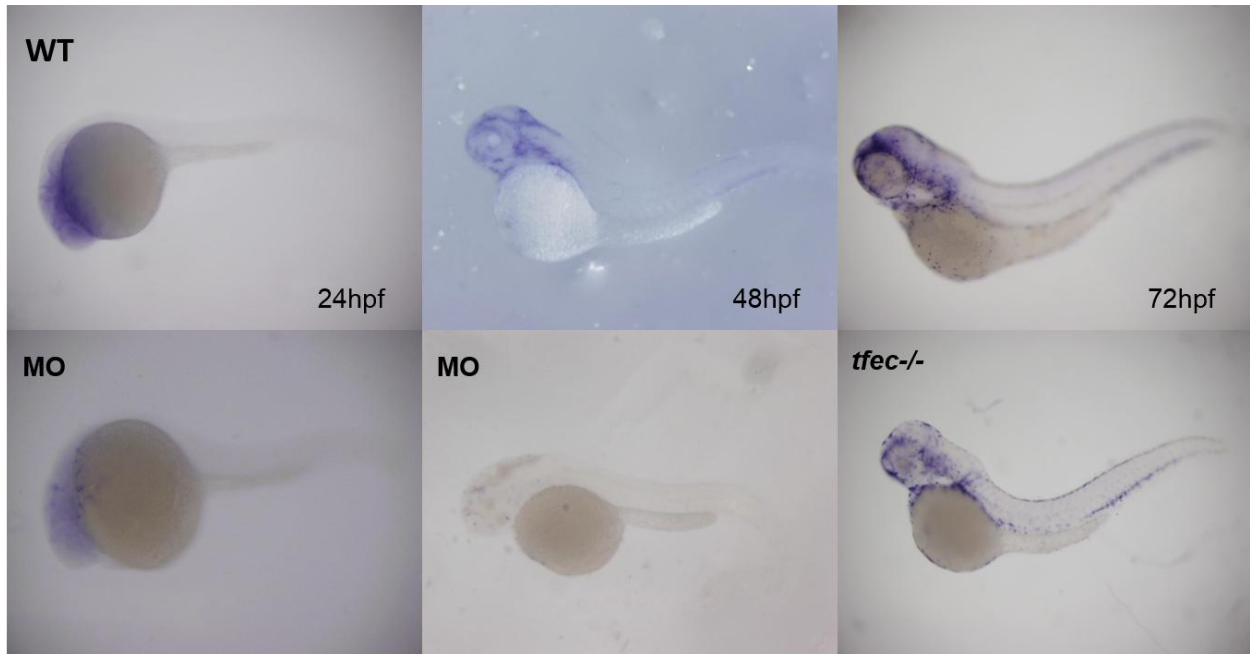


**Figure 20. Delayed expression of *fms* in *tfec* morphants and mutants.** 24hpf embryos showed reduced expression of *fms*, while 48hpf embryos show no expression. 72hpf embryos show reduced expression especially in the head.

### *tfec* mutants show a loss of iridophores

Iridophores are first visible around 42hpf in the developing embryo on the retina (Kimmel et al, 1995). Iridophores continue to fill the eye until they half cover the eye at 72hpf, with the retina visible through radial stripes. Iridophores begin to cover the dorsal stripe by 60hpf and the yolk stripe by 72hpf, with the densest area being the lateral patches on either side of the swim bladder.

Previous data had shown a loss of iridophores at 120hpf in embryos injected with *tfec* morpholinos. Iridophores are absent from the lateral patches and the dorsal and ventral stripes at 96hpf (Figure 21). CRISPR-injected embryos do not develop iridophores in any part of the embryo except the outermost portion of the eye by 120hpf.

A probe, *ltk*, was used to evaluate expression of a marker for iridophores. Leukocyte tyrosine kinase (*ltk* or *shady*) is expressed in the iridophores of zebrafish and are involved in the cell fate specification (Lopes et al, 2008). Mutants of *ltk* have no iridophores in the embryo or adult. Therefore, expression of *ltk* is used as a marker for iridophore development. At 24hpf, the embryos injected with *tfec* CRISPR/Cas9 show no expression of *ltk* while the wild-type controls have expression in the eye and lateral patches (Figure 22). By 48hpf, the embryos show expression of *ltk* in the head and eyes, but no expression in the dorsal or ventral stripes and little expression in the lateral patches. Expression of *ltk* is seen in the eyes, stripes and lateral patches by 72hpf, but expression is fainter in the eyes than compared to the uninjected

embryos. Disruption of the expression of *tfec* causes a loss of iridophore pigmentation in injected embryos and a delay in iridophore development as seen by the *ltk* marker expression.



**Figure 21. Loss of iridophores in *tfec* CRISPR-injected embryos.** Embryos at 96hpf show losses of iridophores in the eyes, lateral patches, and stripes. 120hpf photographs reprinted from Figure 13 for greater magnification of the iridophores of the eye.

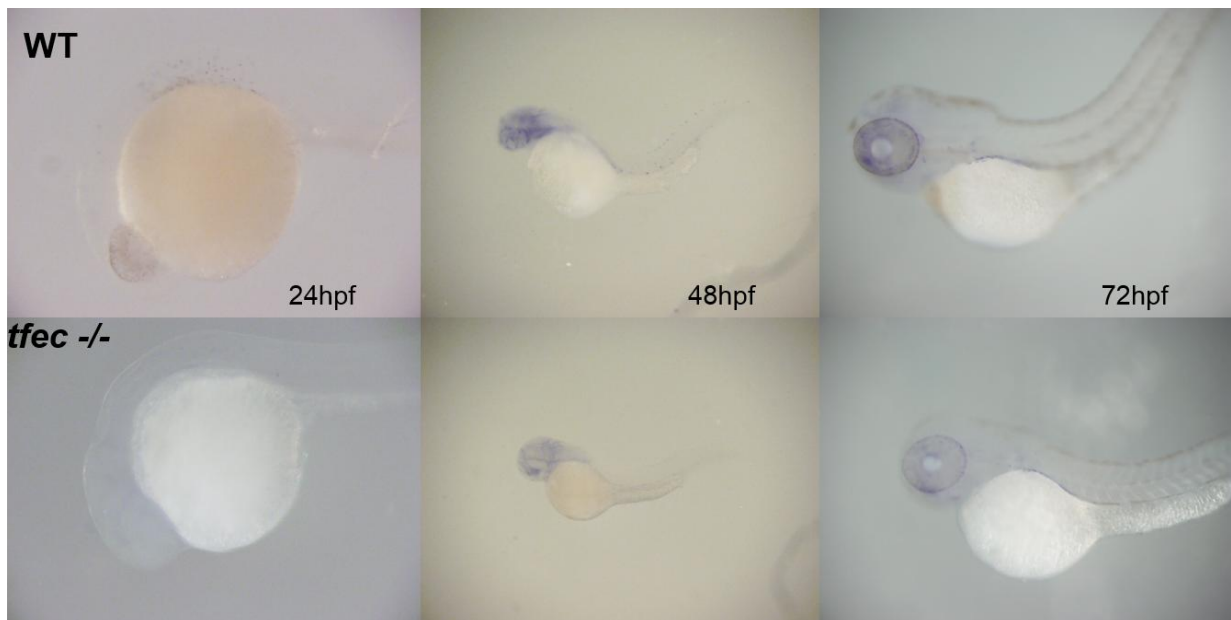


**Figure 22. *tfec* mutants show reduced expression of *ltk*.** Embryos show no *ltk* expression in the eyes or neural crest at 24hpf. At 48hpf reduced expression is seen in the head; however no expression is seen in the lateral patches. At 72hpf reduced expression is seen in the eyes, lateral patches and trunk iridophores.

*tfec* mutations disrupt the organization of trunk melanophores

The larval pigment pattern consists of xanthophores covering the flank and four melanophore stripes. Disruption of larval xanthoblast development does not affect melanophore or iridophore patterning; knockouts of *fms* still retain normal patterning of the other pigment cell types (Quigley and Parichy, 2002). However, disruption of either melanophores or iridophores will disrupt the pattern of the unaffected pigment cell. For example, knockout fish for *mitfa* show increased iridophores no longer localized to stripes (Lister et al, 1999) and knockout fish for *ltk* lose stripe melanophores (Lopes et al, 2008).

Melanophores in the CRISPR-injected embryos showed less organization than in the uninjected wild-type controls. More specifically, the pigmentation of the mutant embryos was patchy and more widespread at 48hpf, with melanophores outside the ventral band, seen as more melanophores throughout the yolk sac (Figure 23). This patterning continued through to 96hpf; by 120hpf, the patterning of melanophores appeared more normal, albeit fainter than in the control embryos. Mutations in *tfec* therefore cause a delay in the correct pattern formation of melanophores.

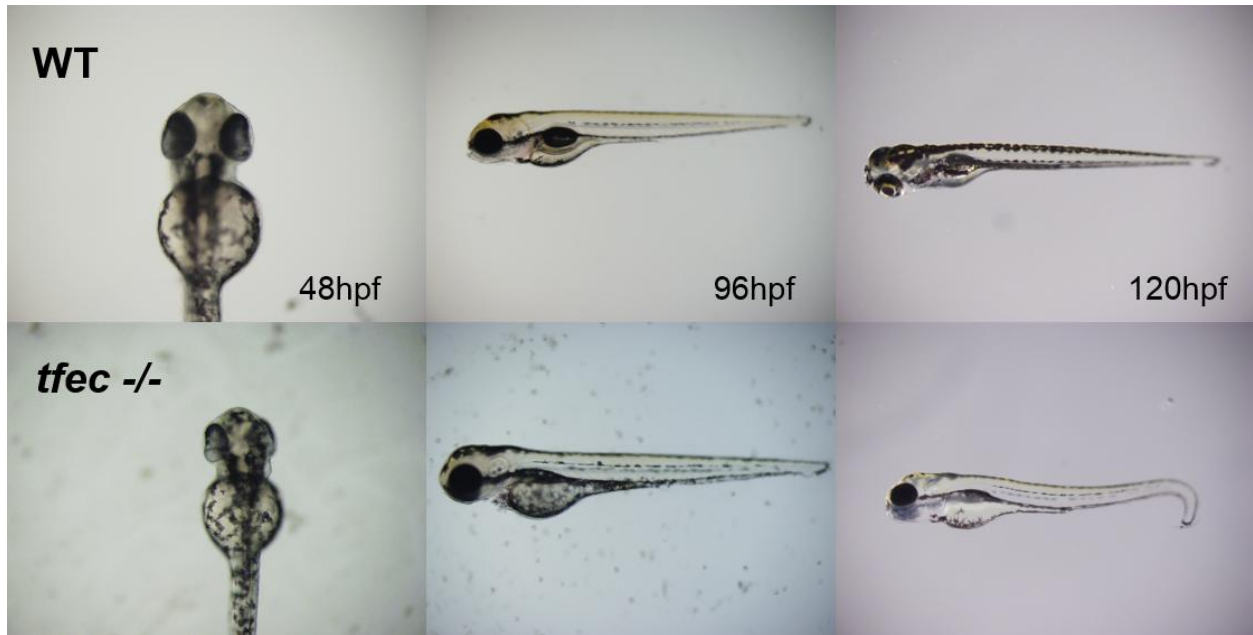


**Figure 23. Loss of *tfec* disrupts melanophore organization.** At 48hpf more melanophores are present on the heads and yolk sacs of CRISPR-injected embryos. At 96hpf, melanophores are seen on the yolk sacs of injected embryos between the ventral and yolk sac stripes, as well as melanophores outside the dorsal stripe on the head. By 96hpf, several melanophores are located above the yolk sac stripe, and melanophores are reduced in the dorsal and lateral stripes.

### ***tfec;mitfa* double mutants lose pigmentation in neural crest and rpe**

*Mitf* null mice show microphthalmia, red eyes and loss of body pigment (Hodgkinson et al, 1993), but loss of function of *Mitf* affects rpe and melanocytes differently. While the melanocytes normally seen in mouse skin and hair follicles are no longer present in *Mitf* null mice, rpe is still present and expresses *dct*; however, there is no expression of tyrosinase and *Tyrp1*, both of which are involved in melanogenesis, so the rpe remains unpigmented (Nakayama et al, 1998). In zebrafish, *mitfa*<sup>w2</sup> mutants lack trunk melanophores and show increased iridophores; however, the rpe is entirely unaffected and still produces normal levels of melanin (Lister et al, 1999; Lane and Lister, 2012). Injection of morpholinos against *tfec* into *mitfa* embryos in previous experiments showed loss of eye pigmentation and iridophores in these embryos; however, the eye pigmentation recovered by 120hpf. In these experiments, morpholinos and CRISPRs were used to generate morphants and mutants of *tfec* in a *mitfa* mutant background. Embryos injected with CRISPR/Cas9 directed against exon 7 of *tfec* were raised for several days and photographed at the following timepoints: 48hpf, 72hpf, 96hpf, and 120hpf. Both morpholino- and CRISPR/Cas9-injected embryos were fixed at several timepoints (24hpf, 48hpf and 72hpf) and *in situ* hybridizations were used to evaluate changes in expression of markers of various tissue types.

*tfec;mitfa* double mutants have abnormal eye shapes

When the optic vesicle invaginates to form the optic cup, the human eye becomes a rounded sphere with the optic stalk coming out and connecting it to the forebrain (Gujar and Gandhi, 2011). In zebrafish, the eyes form similarly, though the final shape is more ovular, especially when viewed dorsally (Li et al, 2000). In the wild-type embryos, the *tfec* mutants and morphants, and the *mitfa* mutant embryos, the eye shapes remained normal, albeit slightly smaller in the *tfec* mutants. The *mitfa;tfec* double mutants at 120hpf show a protrusion of unpigmented tissue in the medial portion of the eye (Figure 24) . The combination of mutations in *tfec* and *mitfa* results in noncircular globes.

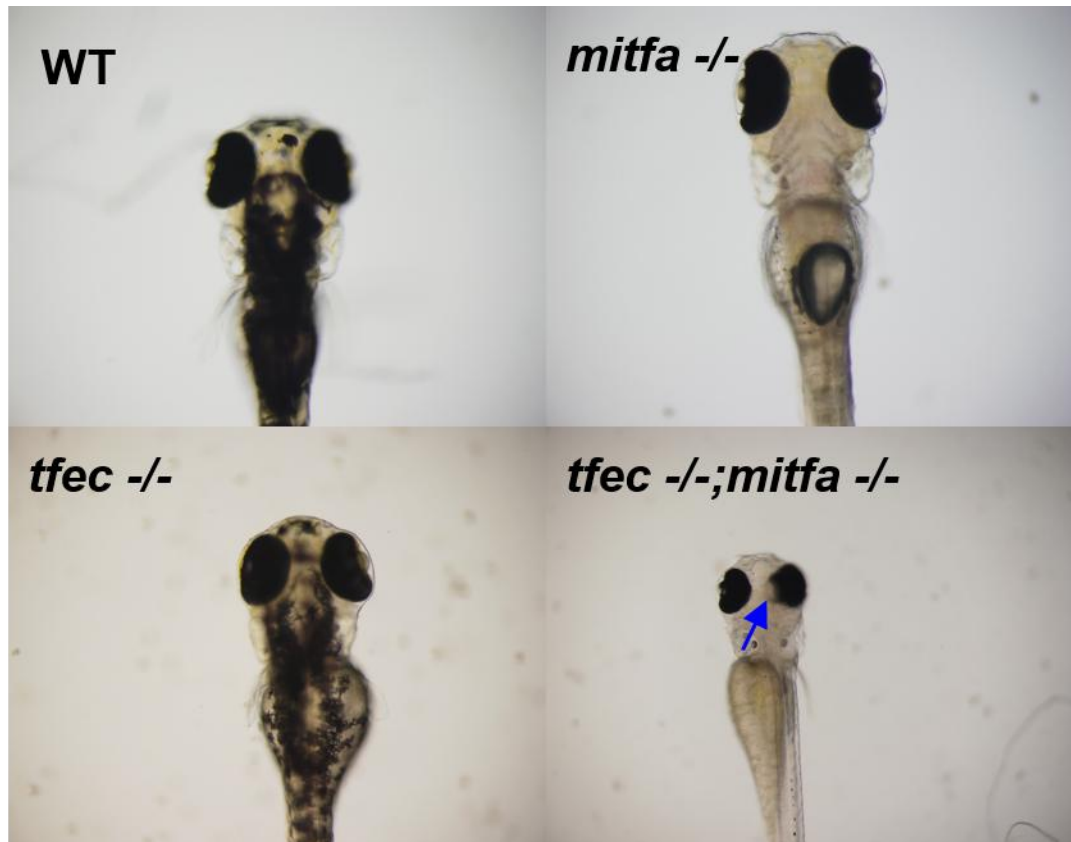


**Figure 24. Double mutants show non-circular ocular globes.** Wild-type embryos injected with CRISPR-Cas9 for *tfec* do not show any deformations in eye shape. *tfec;mitfa* double mutants show unpigmented protrusions from the medial portion of the eye at 120hpf (blue arrow). All embryos with these protrusions showed them bilaterally.

*tfec;mitfa double mutants and morphants show a greater loss of eye melanogenesis*

Mutant fish for *mitfa* show a loss of neural crest-derived melanophores; however, the melanin-producing rpe is unaffected (Lane and Lister, 2012). Previous data had shown reduced eye pigmentation in *mitfa* mutants injected with *tfec* morpholinos (unpublished data). At 48hpf and 72hpf, mutant embryos show a reduction in melanin pigment, especially in the medial portion of the eye (Figure 25). The ring of pigment seen in CRISPR-injected wild-type embryos is also visible in the *mitfa* knockout embryos when injected with the same CRISPR/Cas9. Many of the *mitfa;tfec* embryos had areas of the eye that were missing melanin entirely. By 96hpf, most of the eye pigment recovers, with the exception of colobomas within the iris and the medial portion of the eye. Eye pigmentation is still not fully recovered in the medial portion of the eye by 120hpf, and colobomas are still present. Therefore *tfec;mitfa* double mutants show a more severe loss of melanin pigmentation than *tfec* mutants, especially in the medial region of the eye.

*mitfa* mutant embryos injected with *tfec* morpholinos show a greater reduction in expression of *dct* than *tfec* mutants. Expression of *dct* is still present in the rpe of *mitfa* knockout embryos even though *mitfa* is important for induction of melanogenesis and differentiation of melanophores in zebrafish. At 24hpf, there is no *dct* expression in *tfec*

morphant zebrafish, and at 48hpf and 72hpf, *dct* expression in the eye is less than in wild-type embryos (Figure 26). The loss of *dct* expression is greatest in the medial portion of the eye with no visible probe at any time point. Therefore morphology and *in situ* hybridizations show that mutations in *tfec* and *mitfa* produce a worse phenotype with respect to melanogenesis in the eye than *tfec* mutations alone.

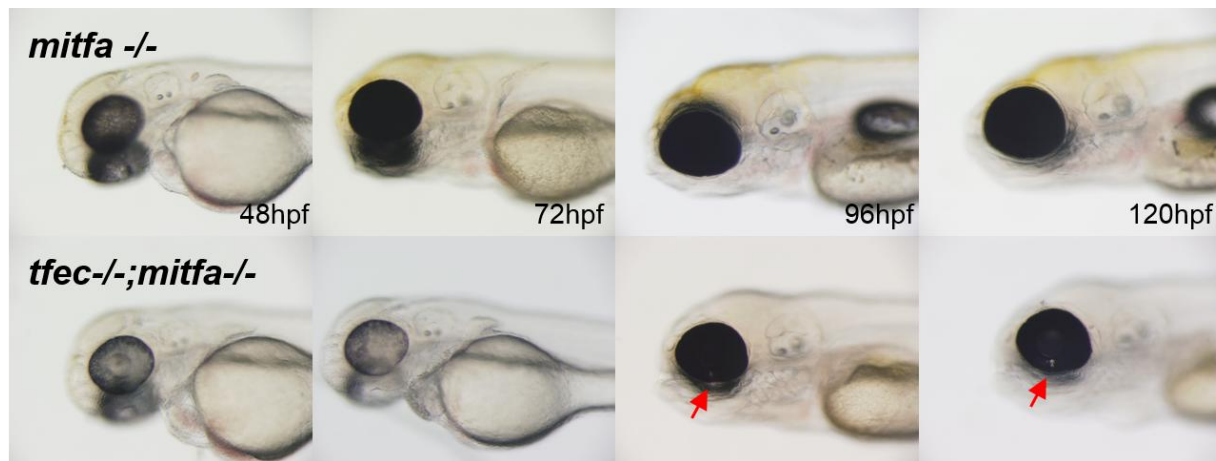


**Figure 25. Double mutants show delayed melanogenesis with loss of melanin in the medial retina and delayed choroid fissure closure.** At 48 and 72hpf, eye pigmentation is reduced, especially in the medial retina. By 96hpf pigmentation has recovered except in the medial retina, seen as unpigmented protrusions from the eye. Colobomas are also seen at 96hpf in injected embryos. By 120hpf pigmentation still has not recovered in the medial retina, and the choroid fissure still has not closed.

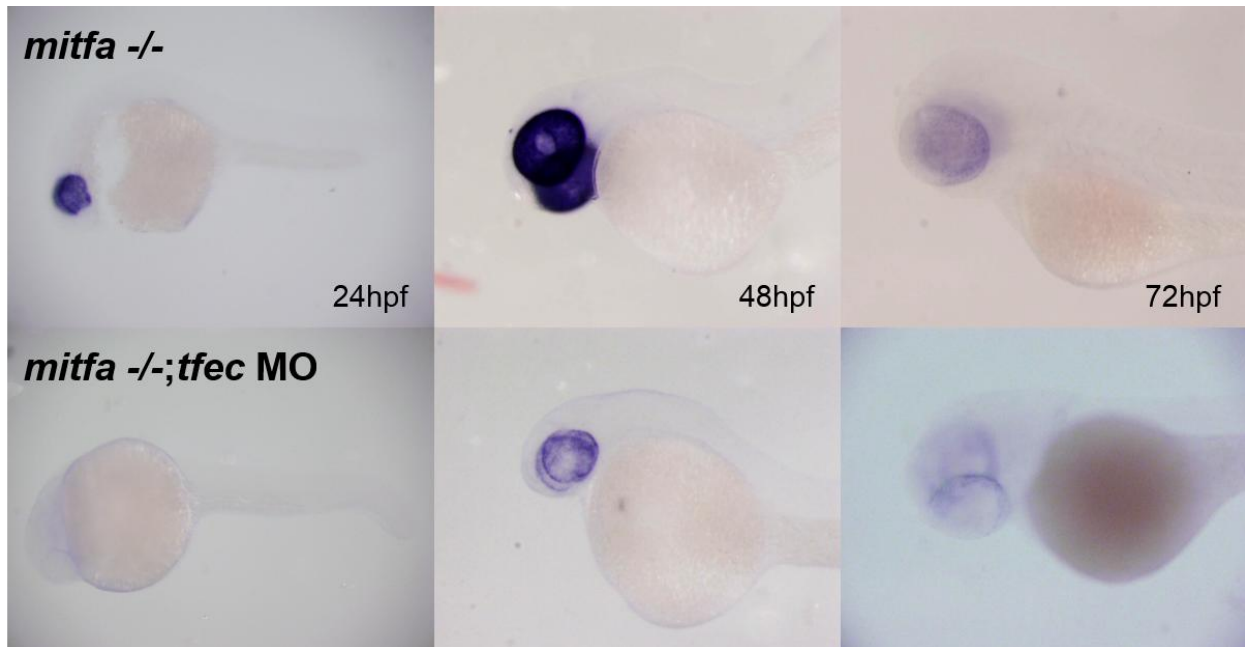


**Figure 26. Double mutants show delayed *dct* expression with a loss of expression from the medial retina.** At 24hpf no *dct* expression is seen. At 48hpf, expression is seen in the peripheral retina. By 72hpf expression is still absent from the medial retina.

Double mutants show a greater loss of rpe

Embryos with mutations in *mitfa* still have rpe; therefore, *mitfa* mutations do not affect expression of *pmelb* or other genes related to melanosome production in the rpe. Injection of *tfec* CRISPR/Cas9 into *mitfa* mutant embryos disrupted expression of the rpe marker *pmelb*. At 24hpf, there is no expression of *pmelb* in injected embryos (Figure 27). At 48 and 72hpf, expression is limited to the lateral retina; no expression is visible in the medial retina. Compared with *tfec* mutant *pmelb* expression, the double mutants show a greater loss of expression, especially in the medial region.

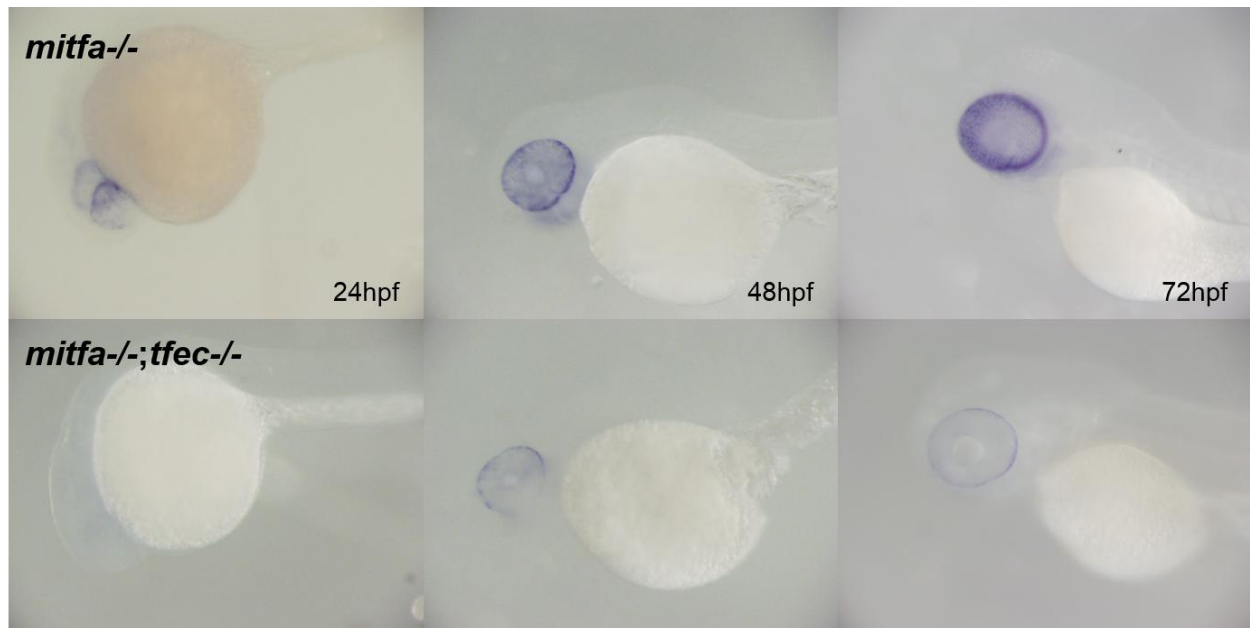


**Figure 27. Double mutants show loss of *pmelb* expression.** At 24hpf, there is no expression of *pmelb*. By 48hpf, expression is present but limited to the peripheral retina. Expression is still limited to the peripheral retina at 72hpf.

*tfec;mitfa double mutants show reduced eye and head size*

Mutations in *MITF*, while causing microphthalmia when homozygous in mice, do not cause microphthalmia in zebrafish. The two orthologs of *MITF*, *mitfa* and *mitfb*, are both expressed in the developing eye, and knockdowns of both do not result in microphthalmia (Lane and Lister, 2012). Furthermore, knockdown of *otx* family of transcription factors results in downregulation of both genes but eye size remains the same, suggesting another transcription factor regulates rpe development. At 5dpf, embryos injected with CRISPR/Cas9 against exon 7 of *tfec* show reduced eye sizes as compared to time matched controls (Figure

25). Furthermore, the head size of the injected embryos seems to also be smaller. Eye size was measured using ImageJ software and plotted as area over time (Figure 28). Additional measurements are needed in order to calculate significance.

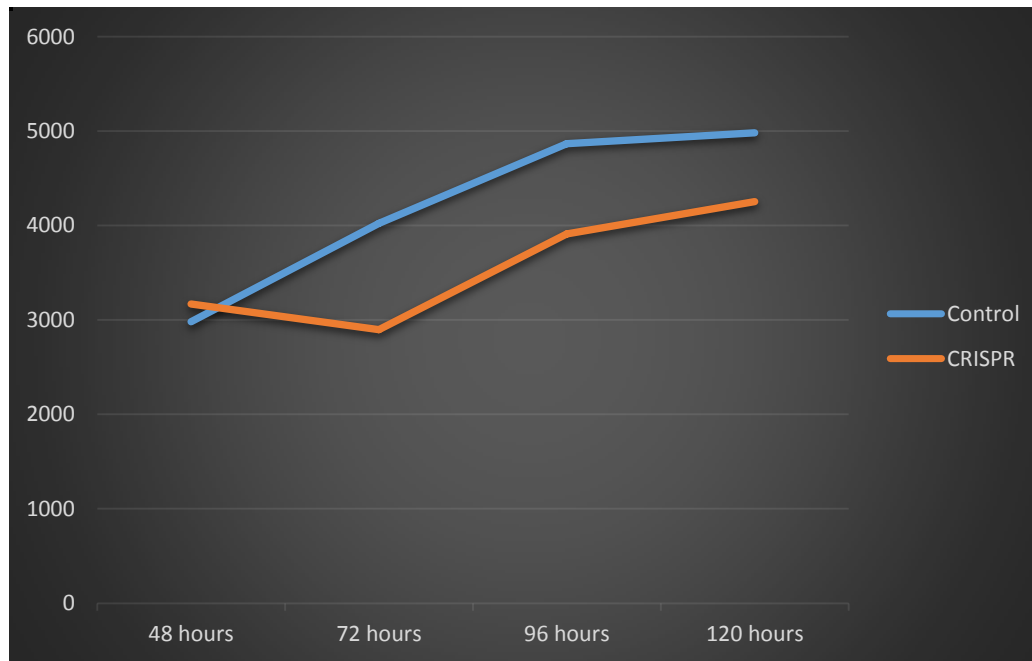


**Figure 28. Eye sizes of CRISPR-injected and control embryos in *mitfa* mutant background.** Eye area was measured in pixels using ImageJ software. At 48hpf, eye sizes are similar. At all other timepoints, eye area was smaller in the CRISPR-injected embryos. Additional measurements are needed to ascertain significance.

*Double mutants lose xanthophore pigmentation*

Zebrafish embryos with mutations in *mitfa* show a reduction in the number of xanthophores, but they are still present (Lister et al, 1999). At 48 hours, pigmentation is visible in the heads of *mitfa* mutant embryos but not in *tfec* CRISPR/Cas9-injected *mitfa* knockout embryos (Figure 29). By 72hpf, no xanthophore pigmentation is seen in the body of injected embryos while full pigmentation is present in uninjected controls, and this lack of pigmentation is visible through 120hpf. This phenotype is more severe than in the *tfec* mutants, where pigmentation in the head was visible by 72hpf and throughout the body by 96hpf. Therefore,

mutations in *tfec* and *mitfa* cause a loss of xanthophore pigmentation whereas *tfec* mutations alone merely cause a delay in xanthopterin pigment.

Expression of both *xdh* and *fms* were used as markers for xanthoblast development. Expression of *xdh* is not visible at 24, 48hpf or 72hpf (Figure 30). At 24hpf, no expression of *fms* is visible, and by 48 and 72hpf, expression is visible but reduced (Figure 31). Marker at 48hpf is visible in the head and the intermediate cell mass. Little probe is visible within the head, and no probe is visible in the trunk at 72hpf. Therefore, *tfec;mitfa* double mutants show a loss of xanthophore pigmentation and a reduction in expression of xanthoblast markers which is more severe than the *tfec* mutants.

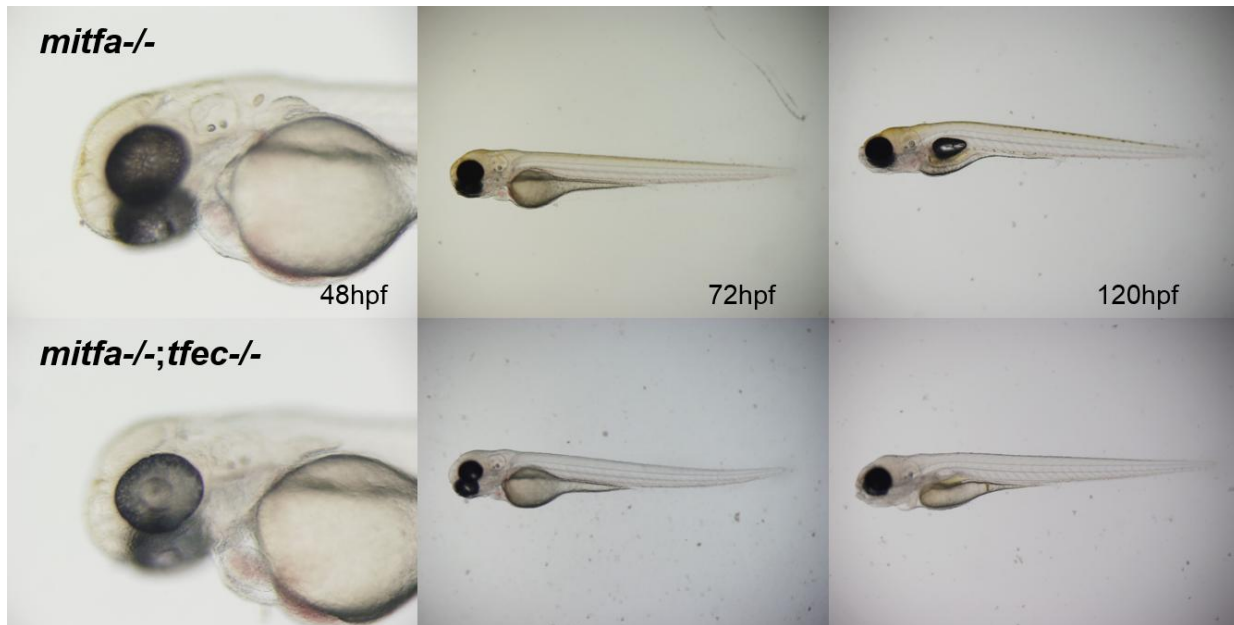


**Figure 29. Loss of xanthophore pigmentation in *tfec* mutants.** At 48hpf, yellow xanthopterin pigment is absent from the heads of double mutants, and pigmentation is absent from the head and trunk at 72hpf and 120 hpf.

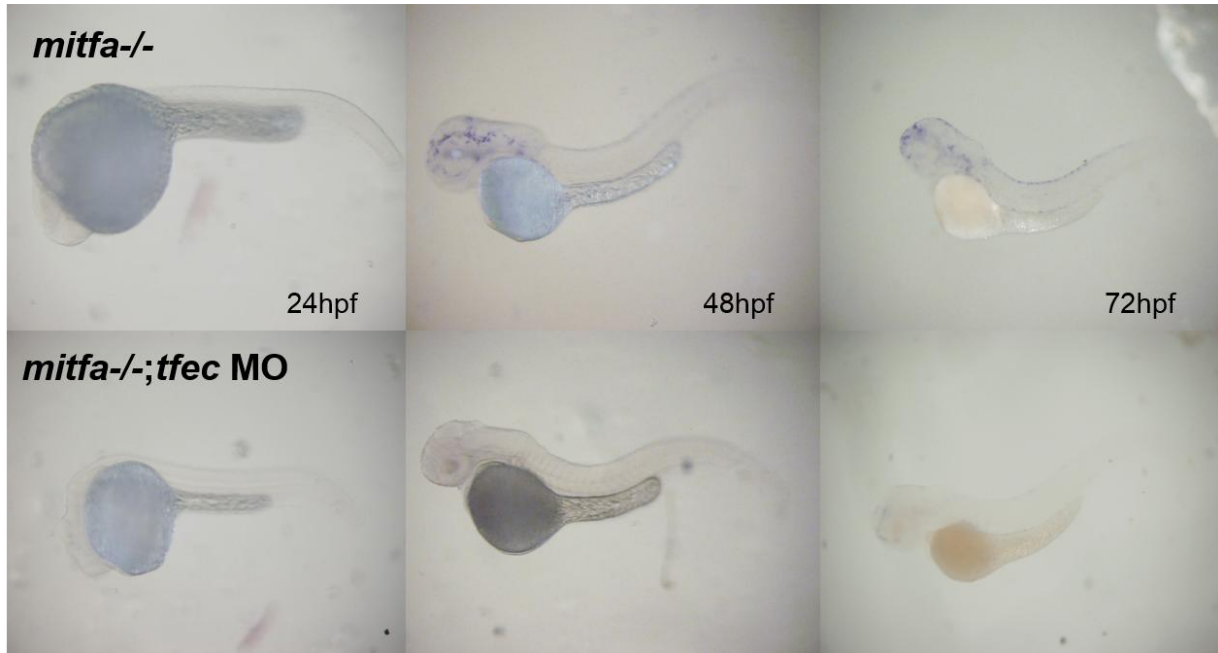


**Figure 30. Loss of *xdh* expression in double mutants.** No expression of *xdh* is visible in 24, 48 or 72hpf embryos.

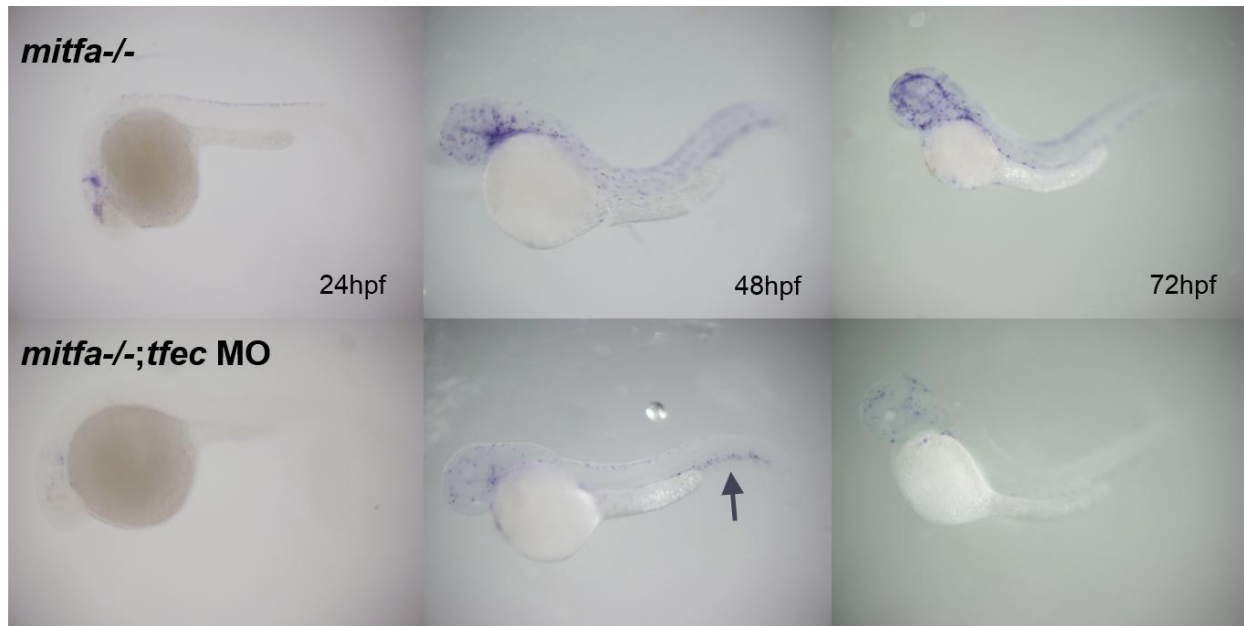


**Figure 31. Loss of *fms* expression in double mutants.** Expression is absent at 24hpf. At 48hpf some expression is visible in the head and the intermediate cell mass (arrow). By 72hpf, little expression is seen the head and no expression is visible in the trunks of injected embryos.

*tfec;mitfa double mutants show a loss of iridophores*

Embryos with mutations in *mitfa* have been shown to have increased numbers of iridophores (Lister et al, 1999). Following injection of CRISPR/Cas9 against *tfec*, embryos had not developed iridophores in the body or eye by 120hpf (Figure 32). Iridophores were absent from the iris, the lateral patches, and the dorsal and ventral stripes.

Expression of the marker *ltk* was used to look at the development of the iridoblast in CRISPR/Cas9-injected embryos. At 24hpf, *ltk* expression is slightly reduced compared to controls (Figure 33). At 48hpf, expression is absent from the lateral patches, an area with dense iridophores, and from the dorsal and ventral stripes. Some expression is visible in the head, mainly in the peripheries of the eyes. By 72hpf, expression in the head is visible but reduced and still primarily limited to the peripheral retina. The lateral patches show some expression, though less than controls, and no expression is visible in the dorsal and ventral

stripes. Mutations in *tfec* disrupt expression of markers for iridoblasts and prevent the development of iridophores in the embryo.



**Figure 32. Loss of iridophores in double mutants.** At 120hpf, iridophores were absent in the eyes, lateral patches and stripes.

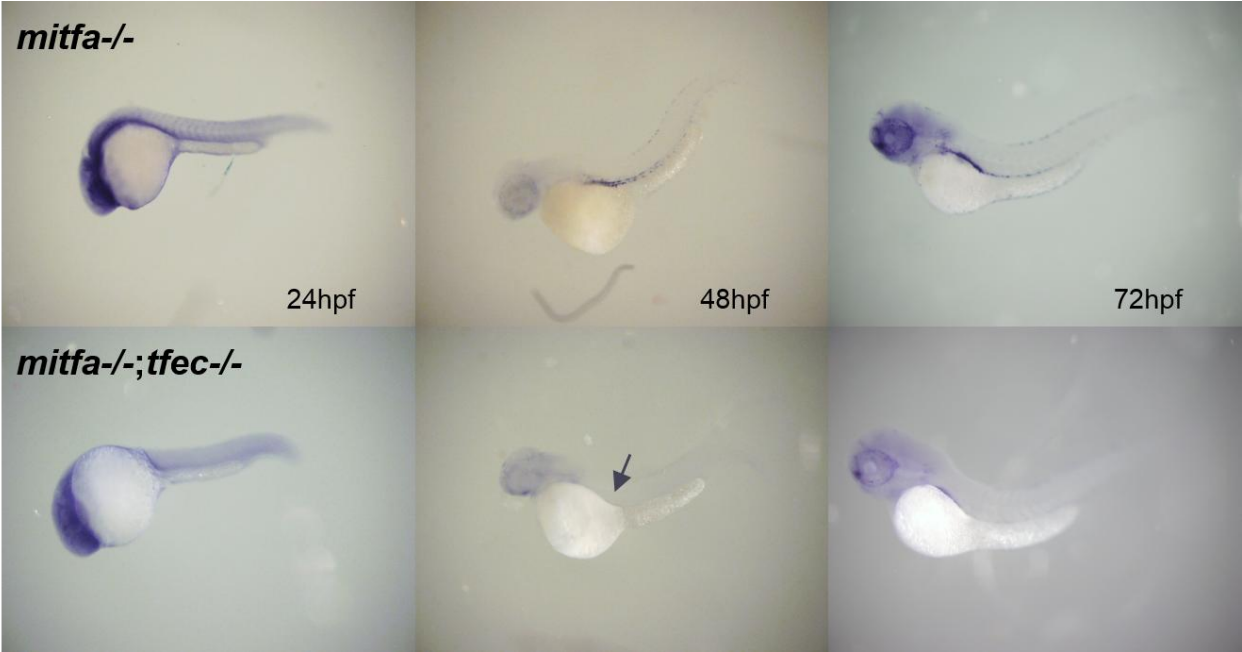


**Figure 33. Reduced expression of *ltk* in double mutants.** At 24hpf, expression was slightly reduced. By 48hpf, expressed was in the head but absent from the lateral patches and stripes. By 72hpf, expression was reduced in the eyes and lateral patches and still absent from the stripes.

#### **Phenotype of exon 8 TALEN-derived mutants**

Embryos from identified carriers were examined for any changes in pigmentation and overall appearance at 48 and 72hpf; by the third day of development, all pigmentation in the embryonic pigment pattern is present in wild-type embryos (Kimmel et al, 1995). Therefore, any changes to pigment cells would be visible by 72hpf.

The F2 embryos from the exon 8 TALENs showed no discernable phenotype (data not shown). Eye pigment developed by normal timepoints as did neural crest-derived pigmentation. Several of these embryos were genotyped, and several were identified as homozygous for *tfec* mutations. However, these embryos were phenotypically no different from heterozygous or homozygous wild-type fish.

#### **Genotyping of exon 3 TALEN-derived mutants**

Embryos from identified germline carriers were raised to generate the first generation (F1) of TALEN-derived fish. These embryos were derived from outcrosses with *mitfa* knockout fish, so embryos were heterozygous for the *mitfa*<sup>w2</sup> mutant allele. The F1 fish were genotyped with fin clip biopsies using PCR and restriction digest. Identified carriers were intercrossed and used to generate second generation (F2) TALEN-derived fish. These embryos were photographed to document their phenotypes for comparison with the CRISPR- and morpholino-injected embryos. Some embryos were also genotyped for mutations in *tfec* and *mitfa* to analyze the correlation between genotype and phenotype. Remaining embryos were raised to

adulthood to generate homozygous mutant adult fish. These adult fish were genotyped using fin clip biopsies and subsequent PCR and restriction digest.

## **CHAPTER 4: DISCUSSION**

### **Pigmentation regulation in zebrafish**

Mammals contain primarily melanin pigments, produced in melanocytes and in the rpe (Cichorek et al, 2013). Mutations affecting pigment production in mammals can have clinical significance. For example, mutations in *PAX3* and *MITF* in humans cause Waardenburg syndrome; these genes regulate the development of neural crest cells from which pigment cells are derived (Read and Newton, 1997). *MITF* specifically is a cell-fate specifying transcription factor that restricts neural crest cells to become melanocytes, and *PAX3* induces expression of *MITF*. Waardenburg syndrome affects approximately 1 in 10,000 people, and symptoms can include pale eyes sometimes with heterochromia, fair skin, white forelock and deafness. Additionally, less skin and iris pigmentation results in individuals being more susceptible to melanomas (Cichorek et al, 2013; Schmidt-Pokrzywniak et al, 2009). The importance of pigment-producing cells in various tissues, including skin, eyes and hair cells of the ear makes them of interest to researchers. While mice have been used for pigment research, it is difficult

to study their early development, especially during the specification, migration and differentiation of the neural crest because it occurs *in utero*.

Pigment production mutations can also cause ocular malformations including microphthalmia and anophthalmia. Heterozygous mutations in murine *Mitf* cause white patches of fur and deafness; homozygous mutations cause loss of fur pigment and microphthalmia because the melanogenesis of the rpe is affected (Hodgkinson et al, 1993). The melanosomes in the rpe degrade toxic substances formed in the retina, including POS with photooxidative damage. Furthermore, the cells of the rpe secrete survival signals like PEDF and FGF to the retina. Without these functions, the retina degrades; however in humans it is difficult to determine which degrades first, the retina (primary degradation) or the rpe (secondary degradation) (Bibliowicz et al, 2011). Therefore animal models are necessary to study retinal degradation.

### **Zebrafish as pigment cell and eye development models**

Zebrafish are excellent models for pigment cell research because they contain multiple types of pigment cells, compared to the singular melanocytes of mammals. Melanophores produce dark melanin pigment, xanthophores produce yellow xanthopterin pigment and iridophores produce iridescent purine plates (Quigley and Parichy, 2002). With these additional pigment cell types, more genetic manipulations are possible that result in visible phenotypes affecting pigmentation and pigment cell development than in mammals where a single pigment cell can be affected. Many transcription factors and enzymes regulate the development of the neural crest into pigment cells; mutations in these can be used to model human disease states.

Furthermore, zebrafish are also useful in studying eye development. The eyes of zebrafish are similar to humans in that both fish and humans are diurnal, and therefore contain more cone photoreceptors than rods (Bibliowicz et al, 2011). As in humans, changes in the rpe affecting its function also impair vision. Because the entire developmental lineage of the eye is visible, primary and secondary retinal degradation can be differentiated by studying zebrafish. Furthermore, the process of choroid fissure closure can be viewed and studied. Therefore, genes in zebrafish can be manipulated using various biotechnologies to study pigment cells during development, including those within the eye, creating models of human diseases.

### **Regulation of pigment cell development**

Melanophores are the most studied of zebrafish chromatophores because of their similarity to previously studied melanocytes in mammals (Quigley and Parichy, 2002). The two homologs of *MITF*, *mitfa* and *mitfb*, have differences in expression; *mitfa* is expressed throughout the body of the zebrafish, while *mitfb* expression is limited to the rpe (Lister et al, 2001). Homozygous mutations in *mitfa* cause loss of neural crest-derived melanophores and an increase in the number of iridophores (Lister et al, 1999). However, this mutant shows no eye-related phenotype as the pigment production of the rpe is unaffected (Lane and Lister, 2012). While *otx* transcription factor morphants show reduced rpe and *otx* members induce *mitfa* and *mitfb*, combined knockdowns of both *mitfa* and *mitfb* do not affect the development nor the melanogenesis of the rpe (Lane et al, 2012). Therefore another transcription factor is thought to regulate melanogenesis within the zebrafish rpe.

The transcription factor *TFEC* was first cloned based on similarity with other MiT family genes within the leucine zipper and helix-loop-helix domains (Zhao et al, 1993). Steingrimsson

et al (2002) found *Tfec* mutant mice were phenotypically normal and did not alter phenotypes of mice mutant for other MiT family members. No human diseases are associated with mutations in *TFEC*. In zebrafish, expression of *tfec* is visible as early as the 8 somite stage within the optic groove and the presumptive neural crest (Lister et al, 2011). Expression continues throughout development in the presumptive rpe and iridoblasts. Embryos injected with morpholinos targeting *tfec* splice sites showed reduced rpe at 48hpf and reduced iridophores at 5dpf (unpublished data).

### **Establishment of several mutant lines for *tfec***

Use of morpholinos for descriptions of novel phenotypes has several disadvantages, including temporary effects and phenotypes that do not match those of mutants (Nasevicius and Ekker, 2000; Schulte-Merker and Stainier, 2014; Kok et al, 2015). The recovery of the rpe by 5 days may have been because *tfec* expression is critical during a certain time during development or because the morpholinos were being degraded. Therefore the creation of a line of zebrafish mutant for mutant for *tfec* was of interest to study the long-term effects of *tfec* depletion and to corroborate the morphant phenotype.

To this end, TALENs or CRISPR/Cas9 systems were used to generate embryos with mosaic mutations for *tfec*. Two TALENs were separately used against exons 8 and 3, and one CRISPR gRNA was designed against exon 7. Several of these mutations were in-frame, and therefore were not predicted to have any major effect on the structure of the protein. Other mutations resulted in early stop codons, and these were predicted to have deleterious effects on the stability of *tfec*. However, none of these mutations result in a dominant negative species.

The original *microphthalmia* mutant in mice shows a deletion of a single arginine of four conserved arginines in the DNA binding domain (Hodgkinson et al, 1993). The helix-loop-helix domain possesses a basic region in the first alpha helix that contacts the DNA; the deletion of the arginine from the basic region prevents DNA binding but does not affect the remaining structure, allowing the mutant protein to form homo- and heterodimers. The mutant Mitf protein creates dominant negative species where dimers form but cannot activate transcription. The mutations in *tfec*, while deleterious in function, would not affect the DNA binding domain in the fifth exon, and therefore would not result in the more severe dominant negative mutations (Lister et al, 2011).

#### ***tfec* positively regulates development of iridophores, xanthophores and rpe**

Wild-type embryos were injected with morpholinos directed against *tfec* to study the role of *tfec* in pigment cell development, both in the rpe and the neural crest. Embryos were also injected with CRISPR/Cas9 for exon 7 of *tfec* to corroborate the phenotype seen previously with morpholinos.

Both *tfec* morphants and mutants showed delays in the development of iridophores, xanthophores, melanophores and rpe. While pigmentation of all cell types is typically visible by 48hpf, especially within the head, pigmentation was reduced in the rpe until 96hpf. This pigmentation delay appeared to be a result of inability to produce melanosomes, as both *pmelb* and *dct* expression was affected. Reduction in melanogenesis may have delayed eye growth during development. For example, mutations in *pmelb* results in hypopigmentation of the rpe and toxic buildup of undigested POS, causing microphthalmia (Bibliowicz et al, 2012). The hypopigmentation is a result of an inability of melanosomes to mature (Schonthaler et al,

2005). Therefore the decreased pigmentation in *tfec* morphants and mutants may have affected the growth and development of both the rpe and the retina.

Pigmentation was also lacking in xanthophores at 48hpf; however they developed pigmentation by 96hpf. Because the pigmentation eventually appears in the correct location, *tfec* mutations affect neither the specification nor migration of xanthoblasts. The lack of pigmentation at 48 and 72hpf could have multiple causes: either the xanthoblasts are differentiating but failing to produce pigment, or the xanthoblasts failed to differentiate and therefore no pigment would be produced (Kelsh et al, 1996). The expression of two markers for xanthoblasts, *fms* and *x dh*, were also affected; this implies an initial failure of the chromatoblasts to differentiate into xanthoblasts, and therefore resulting in a delay in pigmentation. This delay in xanthophore pigmentation suggests roles for other transcription factors later in pigment cell development.

Iridophores failed to develop by 120hpf in the eyes, the lateral patches, and the dorsal, ventral and yolk stripes. As with the xanthophores, this pigmentation loss could be due to either failure to differentiate or lack of transcription of pigmentation genes. The expression of the marker *ltk* was disrupted; this suggests that *tfec* regulates the differentiation of iridophores, and disruption of its expression caused the visible loss of pigmentation. However, unlike with the rpe and xanthophores, no other transcription factor compensated for *tfec* in its function so the iridophores failed to differentiate rather than simply be delayed.

Melanophores were seen between the ventral and yolk stripes on the yolk sac where these cells are normally restricted to these stripes by 120hpf. Loss of cell-cell contacts from iridophores may have resulted in erroneous pattern formation (Quigley and Parichy, 2002).

Interestingly, while melanogenesis in the eyes recovers by 96hpf, the closure of the choroid fissure is affected as evidenced by the colobomas within these embryos. The choroid fissure usually closes around 72hpf (Kimmel et al, 1995); *tfec* mutant embryos have delayed choroid fissure closure sometime between 96 and 120hpf. Colobomas result when the edges of the developing optic cup fail to fuse by the correct timepoint (Bibliowicz et al, 2011). Previously identified genes causing colobomas in zebrafish affect the development of the optic cup, both within the retinal and rpe layers. Another transcription factor family, *otx*, particularly *otx2*, has been shown to have a role in the development of the rpe in zebrafish; mutations in *otx2* results in colobomas (Lane and Lister, 2012; Bharathan, 2014). Therefore, the *otx* transcription factors may be compensating for *tfec* loss in rpe pigmentation, leading to delayed but successful fusion of the choroid fissure.

#### ***tfec* and *mitfa* cooperatively regulate rpe, iridophore and xanthophore development**

Preliminary data showed *mitfa* mutant embryos injected with *tfec* morpholinos had a greater loss of pigmentation in the rpe and iridophores. Embryos homozygous for the *mitfa*<sup>w2</sup> allele were injected with CRISPR-Cas9 and morpholinos against *tfec* and showed double mutants display a more severe phenotype as compared with *tfec* mutations alone.

CRISPR-Cas9 generated mutants showed greater delays in pigmentation of xanthophores, iridophores, and rpe. The loss of pigmentation in the eyes at 48hpf is greater in *mitfa;tfec* double mutants than in *tfec* mutants, and melanin absence is greatest in the medial retina. Eye melanogenesis is delayed until 96hpf, and even at 120hpf the eyes remain small compared to controls with protusions that remain unpigmented. The eventual development of pigmentation outside the medial retina may be due to *mitfb*, which is expressed in the rpe

though it does not lead to pigment loss in morphants, or to *otx* family transcription factors which are expressed in the rpe and regulate transdifferentiation of retina into rpe, or to another factor entirely (Lane and Lister, 2012; Bharathan, 2014). The role of both of these proteins in rpe differentiation is also reflected in marker expression data. *mitfa*<sup>w2</sup> embryos injected with *tfec* morpholinos or CRISPR/Cas9 showed a greater loss of *dct* or *pmelb* expression, respectively, at 72hpf within the medial retina where melanin pigmentation was also most affected. While *tfec* morphants and mutants showed a delay in both of these markers, *mitfa;tfec* double mutants appear to have a loss of expression altogether, suggesting a failure of rpe to differentiate in the medial retina.

Pigmentation from xanthophores was not visible by 120hpf. As xanthophore numbers are reduced in both of the single mutants, yet absent in the double mutants, this suggests these transcription factors cooperate in their regulation of the differentiation of xanthophores. Expression of *xdh* and *fms* were absent or nearly absent in morphant and mutant embryos at 72hpf, corresponding with the loss of xanthophore pigmentation at all timepoints due to a lack of differentiation of chromatoblasts into xanthophores. Therefore *mitfa* expression in the *tfec* single mutants resulted in the delayed pigmentation of xanthophores.

Iridophore pigmentation was also not visible by 120hpf, similar to what was seen in the single mutants. In *mitfa;tfec* mutant embryos *ltk* expression was greatly reduced in the heads and lateral patches of 72hpf embryos and was absent from the stripe iridophores, as was seen in the single mutants. Therefore, mutations in *mitfa* do not affect the iridophore phenotype seen in *tfec* mutants.

Choroid fissure closure is also more affected in the double mutants. While the *tfec* mutants showed choroid fissure closure by 120hpf, *mitfa;tfec* double mutants do not. This phenotype is reflective of the greater deficit in the differentiation of the rpe.

Overall, the pigmentation loss seen in the embryos with mutations in both *tfec* and *mitfa* was greater than in embryos with *tfec* mutations alone. Also the pigmentation loss appears to be more permanent, as compared with delays in pigmentation seen in the single mutants. This longer-lasting phenotype may be due to an interaction of *mitfa* and *tfec* during pigment cell differentiation.

## Conclusions

The experiments performed in this study aimed at characterizing the role of *tfec*, an MIT family member, in zebrafish pigment cell development, specifically the rpe of the eye and the neural-crest derived pigment cells: xanthophores, iridophores and melanophores, as well as determining its interactions with *mitfa*, a melanophore cell-fate specifier.

Loss of *tfec* alone caused delays in pigmentation of xanthophores and rpe as well as loss of iridophore pigmentation from larvae. Mutations in *tfec* also caused colobomas, implying a role in the regulation of choroid fissure closure, perhaps with *otx* family members. The transcription factor *tfec* appears to have a role in specification of iridoblasts; loss of iridoblasts appears to affect development of the other pigment cells, perhaps via cell-cell contacts.

Double mutants for *tfec* and *mitfa* showed a greater delay in pigmentation of the rpe, with noncircular ocular globes having protrusions in the medial retina with no pigment. Specification of the rpe is regulated by *mitfa* and *tfec* cooperatively with potential contribution from *mitfb*; however, *mitfa* and *mitfb* have minor roles in melanogenesis of the rpe while *tfec*

has a larger role in rpe specification. Embryos with *mitfa;tfec* mutations also showed a loss of xanthophore pigmentation, implying a cooperative role of *mitfa* and *tfec* in xanthoblast specification. These embryos additionally showed a loss of iridophore pigmentation, suggesting *tfec* positively regulates iridoblasts while *mitfa* induces bipotential chromatoblasts to become melanophores; mutations in *mitfa* alone result in an increase in iridophores and a loss of melanophores. Double mutants displayed colobomas which did not close at any of the timepoints photographed, implying a role for both transcription factors in regulating choroid fissure closure. Therefore, *tfec* and *mitfa* cooperatively regulate specification of multiple pigment cells, including xanthophores and the rpe, but are not critical for rpe development, as melanin pigment develops in the eyes of both single and double mutants.

Based on the morphology and expression of markers, I have created a model for the roles of *tfec* and *mitfa* in pigment cell differentiation (Figure 34). The relative sizes of the arrows denote the impact of the mutation on that pigment cell type. Because mutations in *mitfa* result in loss of neural crest-derived melanophores and decreases in xanthophores, differentiation of these cells is regulated by *mitfa* (Lister et al, 1999). While *mitfa* is expressed in the rpe, and may have some role in regulating the ectoderm-derived melanophores, mutants do not show a visible rpe phenotype (Lane and Lister, 2012). Both single and double mutants for *tfec* show loss of iridophore pigmentation and marker expression of *ltk*; therefore *tfec* plays a large role in the differentiation of iridophores while *mitfa* does not. The additional iridophores seen in *mitfa* mutants are probably a result of increased numbers of undifferentiated chromatoblasts being fated as iridophores. Double mutants for *tfec* and *mitfa* show greater pigment losses in the rpe and xanthophores than single mutants; therefore these

transcription factors interact when regulating the differentiation of these cells. The pigmentation seen in the peripheral retina is possibly a result of other transcription factors, including *mitfb*, *otx1a*, *otx1b* or *otx2*. Additional testing of this model would include markers for earlier portions of the development of the neural crest to identify the role of these proteins in cell fate specification, as well as creation of an overexpression transgene for *tfec*, which one would expect to have increases in xanthophores and iridophores with fewer changes to melanophores or rpe.

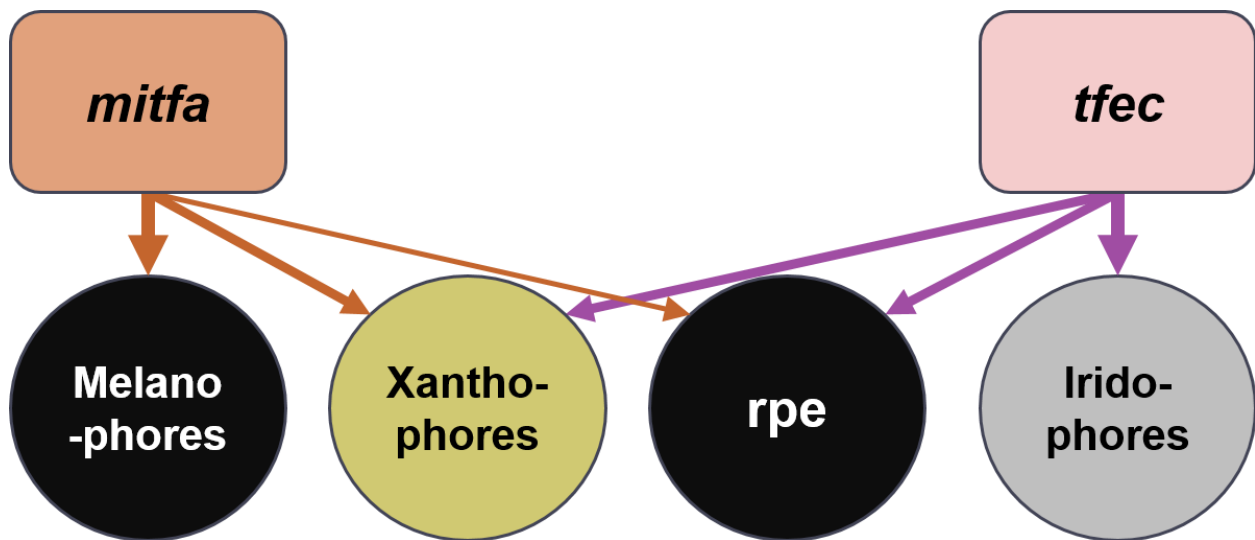


**Figure 34. Model of the roles of *mitfa* and *tfec* in pigment cell differentiation.** Arrow size denotes the relative importance of each protein in the development of these cell types.

### LITERATURE CITED

Alaluf S, Atkins D, Barrett K, Blount M, Carter N, Heath A. Ethnic variation in melanin content and composition in photoexposed and photoprotected human skin. *Pigment Cell Research*. 2002; 15(2):112-118.

Basch ML, García-Castro MI, Bronner-Fraser M. Molecular mechanisms of neural crest induction. *Birth Defects Research Part C: Embryo Today: Reviews*. 2004; 72(2):109-123.

Bharathan, NK. The role of the rx3/otx pathway in zebrafish eye development. [Master's thesis]. Richmond, VA: Virginia Commonwealth University. 2014.

Bharti K, Gasper M, Ou J, Brucato M, Clore-Gronenborn K, Pickel J, Arnheiter H, and Van Heyningen V. A Regulatory Loop Involving PAX6, MITF, and WNT Signaling Controls Retinal Pigment Epithelium Development (PAX6 and Mi-T Members in RPE Development). *PLoS Genetics*. 2012; 8, no. 7: E1002757.

Bibliowicz J, Tittle RK, Gross JM. Toward a better understanding of human eye disease insights from the zebrafish, *danio rerio*. *Progress in molecular biology and translational science*. 2011; 100:287.

Boch J, Bonas U. Xanthomonas AvrBs3 family-type III effectors: Discovery and function. *Annu Rev Phytopathol.* 2010; 48:419-436.

Bondurand N, Pingault V, Goerich DE, Lemort N, Sock E, Le Caignec C, Wegner M, and Goossens M. Interaction between SOX10, PAX3 and MITF, Three Genes Altered in Waardenburg Syndrome. *American Journal Of Human Genetics.* 2000; 67, no. 4: 194.

Brouns SJJ, Jore MM, Lundgren M, et al. Small CRISPR RNAs guide antiviral defense in prokaryotes. *Science.* 2008; 321(5891):960-964.

Cermak T, Doyle EL, Christian M, et al. Efficient design and assembly of custom TALEN and other TAL effector-based constructs for DNA targeting. *Nucleic Acids Res.* 2011; 39(12):e82-e82.

Cichorek M, Wachulska M, Stasiewicz A. Heterogeneity of neural crest-derived melanocytes. *Cent eur j biol.* 2013; 8(4):315-330.

Colas J, Schoenwolf GC. Towards a cellular and molecular understanding of neurulation. *Developmental Dynamics.* 2001; 221(2):117-145.

Duband JL. Neural Crest Delamination and Migration: Integrating Regulations of Cell Interactions, Locomotion, Survival and Fate. Madame Curie Bioscience Database [Internet]. Austin (TX): Landes Bioscience; 2000.

Eisen JS, Weston JA. Development of the neural crest in the zebrafish. *Dev Biol.* 1993; 159(1):50-59.

Elworthy S, Lister JA, Carney TJ, Raible DW, and Kelsh RN. Transcriptional Regulation of Mitfa Accounts for the Sox10 Requirement in Zebrafish Melanophore Development. *Development*. 2003; 130, no. 12: 2809-18.

Gujar SK, Gandhi D. Congenital malformations of the orbit. *Neuroimaging clinics of North America*. 2011; 21(3):585-602, viii.

Hellstrom A, Watt B, Fard SS, et al. Inactivation of pmel alters melanosome shape but has only a subtle effect on visible pigmentation. *Plos Genetics; PLoS Genet*. 2011; 7(9).

Hemesath T. Microphthalmia, a critical factor in melanocyte development, defines a discrete transcription factor family. *Genes & development*. 1994; 8:2770-2780.

Hodgkinson CA, Moore KJ, Nakayama A, et al. Mutations at the mouse microphthalmia locus are associated with defects in a gene encoding a novel basic-helix-loop-helix-zipper protein. *Cell*. 1993; 74(2):395-404.

Jao L, Wente S, Chen W. Efficient multiplex biallelic zebrafish genome editing using a CRISPR nuclease system. *Proc Natl Acad Sci U S A*. 2013; 110(34):13904-13909.

Johnson S, Nguyen A, Lister J. Mitfa is required at multiple stages of melanocyte differentiation but not to establish the melanocyte stem cell. *Dev Biol*. 2011; 350(2):405-413.

Kimmel CB, Ballard WW, Kimmel SR, Ullmann B, and Schilling TF. Stages of embryonic development of the zebrafish. *Developmental Dynamics* 203, no. 3 (1995): 253-310.

Kelsh RN, Eisen JS. The zebrafish colourless gene regulates development of non-ectomesenchymal neural crest derivatives. *Development*. 2000; 127(3):515.

Kelsh RN, Harris ML, Colanesi S, Erickson CA. Stripes and belly-spots—A review of pigment cell morphogenesis in vertebrates. *Semin Cell Dev Biol.* 2009; 20(1):90-104.

Kelsh RN, Brand M, Jiang YJ, et al. Zebrafish pigmentation mutations and the processes of neural crest development. *Development.* 1996;123:369.

Kelsh RN, Schmid B, Eisen JS. Genetic analysis of melanophore development in zebrafish embryos. *Dev Biol.* 2000; 225(2):277-293.

Kleinjan DA, Bancewicz RM, Gautier P, Dahm R, Schonhaler HB, Damante G, Seawright A, Hever AM, Yeyati PL, Van Heyningen V, and Coutinho P. Subfunctionalization of Duplicated Zebrafish Pax6 Genes by Cis-regulatory Divergence. *Plos Genetics.* 2008; 4, no. 2.

Kok F, Shin M, Ni C, Gupta A, Grosse A, Van impel A, Kirchmaier B, Peterson-Maduro J, Kourkoulis G, Male I, Desantis D, Sheppard-Tindell S, Ebarasi L, Betsholtz C, Schulte-Merker S, Wolfe S, and Lawson N. Reverse Genetic Screening Reveals Poor Correlation between Morpholino-Induced and Mutant Phenotypes in Zebrafish. *Developmental Cell.* 2015; 32, no. 1: 97-108.

Kolb H, Fernandez E, Nelson R. The Organization of the Retina and Visual System. *Webvision: the organization of the retina and visual system.* National Library of Medicine: National Center for Biotechnology Information; NCBI; 2012.

Lane BM, Lister JA. Otx but not mitf transcription factors are required for zebrafish retinal pigment epithelium development. 2012; 7(11):e49357.

Le HT, Dowling JE, Cameron DJ. Early retinoic acid deprivation in developing zebrafish results in microphthalmia. 2012; 29(4-5):219-228.

Li Z, Joseph N, Easter SS. The morphogenesis of the zebrafish eye, including a fate map of the optic vesicle. *Dev Dyn*. 2000; 218(1):175-188.

Lin J, Fisher D. Melanocyte biology and skin pigmentation. *Nature*. 2007; 445(7130):843-850.

Lister J, Robertson CP, Lepage T, Johnson S, Raible D. Nacre encodes a zebrafish microphthalmia-related protein that regulates neural-crest-derived pigment cell fate. *Development*. 1999; 126(17):3757-3767.

Lister JA, Lane BM, Nguyen A, Lunney K. Embryonic expression of zebrafish MiT family genes *tfe3b*, *tfeb*, and *tfec*. *Developmental Dynamics*. 2011; 240(11):2529-2538.

Lopes SS, Yang X, Müller J, et al. Leukocyte tyrosine kinase functions in pigment cell development (LTK in pigment cell fate specification). *PLoS Genetics*. 2008; 4(3):e1000026.

Ramón Martínez-Morales J, Rodrigo I, and Bovolenta P. Eye development: a view from the retina pigmented epithelium. *Bioessays*. 2004; 26: 766–777. doi: 10.1002/bies.20064

Minchin JEN, Hughes SM. Sequential actions of Pax3 and Pax7 drive xanthophore development in zebrafish neural crest. *Dev Biol*. 2008; 317(2):508-522.

Moscou MJ, Bogdanove AJ. A simple cipher governs DNA recognition by TAL effectors. *Science*. 2009; 326(5959):1501-1501.

Murisier F, Guichard S, and Beermann F. A Conserved Transcriptional Enhancer That Specifies *Tyrp1* Expression to Melanocytes. *Developmental Biology*. 2006; 298, no. 2: 644-55.

Nakayama A, Nguyen M, Chen C, Opdecamp K, Hodgkinson C, Amheiter H. Mutations in microphthalmia, the mouse homolog of the human deafness gene MITF, affect neuroepithelial and neural crest-derived melanocytes differently. *Mech Dev.* 1998; 70(1-2):155-166.

Nasevicius A, Ekker SC. Effective targeted gene 'knockdown' in zebrafish. *Nat Genet.* 2000; 26(2):216.

Nishiwaki Y, Komori A, Sagara H, et al. Mutation of cGMP phosphodiesterase 6 $\alpha'$ -subunit gene causes progressive degeneration of cone photoreceptors in zebrafish. *Mech Dev.* 2008; 125(11):932-946.

Nornes S, Clarkson M, Mikkola I, et al. Zebrafish contains two Pax6 genes involved in eye development1. *Mech Dev.* 1998; 77(2):185-196.

Parichy DM, Ransom DG, Paw B, Zon LI, Johnson SL. An orthologue of the kit-related gene *fms* is required for development of neural crest-derived xanthophores and a subpopulation of adult melanocytes in the zebrafish, *danio rerio*. *Development.* 2000; 127(14):3031.

Patterson LB, Parichy DM. Interactions with iridophores and the tissue environment required for patterning melanophores and xanthophores during zebrafish adult pigment stripe formation (cellular interactions in stripe development). . 2013; 9(5):e1003561.

Purves D, Augustine GJ, Fitzpatrick D, et al., editors. The Initial Formation of the Nervous System: Gastrulation and Neurulation. Neuroscience. 2nd edition. Sunderland (MA): Sinauer Associates; 2001.

Quigley IK, Parichy DM. Pigment pattern formation in zebrafish: A model for developmental genetics and the evolution of form. *Microsc Res Tech.* 2002; 58(6):442-455.

Raviv S, Bharti K, Rencus-Lazar S, et al. PAX6 regulates melanogenesis in the retinal pigmented epithelium through feed-forward regulatory interactions with MITF. *Plos Genetics*. 2014; 10(5).

Read AP, Newton VE. Waardenburg syndrome. *J Med Genet*. 1997; 34(8):656.

Rehli M, Sulzbacher S, Pape S, et al. Transcription factor tfec contributes to the IL-4-inducible expression of a small group of genes in mouse macrophages including the granulocyte colony-stimulating factor receptor. *The journal of immunology*. 2005; 174(11):7111-7122.

Rowan S, Chen CA, Young TL, Fisher DE, Cepko CL. Transdifferentiation of the retina into pigmented cells in ocular retardation mice defines a new function of the homeodomain gene Chx10. *Development*. 2004; 131(20):5139.

Sander JD, Cade L, Khayter C, et al. Targeted gene disruption in somatic zebrafish cells using engineered TALENs. *Nat Biotechnol*. 2011; 29(8):697-698.

Schmidt-Pokrzywniak A, Jöckel K, Bornfeld N, Sauerwein W, Stang A. Positive interaction between light iris color and ultraviolet radiation in relation to the risk of uveal melanoma: A case-control study. *Ophthalmology*. 2009; 116(2):340-348.

Schonthaler HB, Lampert JM, von Lintig J, Schwarz H, Geisler R, Neuhauss SCF. A mutation in the silver gene leads to defects in melanosome biogenesis and alterations in the visual system in the zebrafish mutant fading vision. *Dev Biol*. 2005; 284(2):421-436.

Schulte-Merker S, Stainier D. Out with the old, in with the new: Reassessing morpholino knockdowns in light of genome editing technology. *Development*. 2014; 141(16):3103-3104.

Steiner CC, Römpler H, Boettger LM, Schöneberg T, and Hoekstra HE. The Genetic Basis of Phenotypic Convergence in Beach Mice: Similar Pigment Patterns but Different Genes. *Mol Biol Evol* (2009) 26 (1): 35-45.

Steingrimsson E, Tessarollo L, Pathak B, Hou L, Arnheiter H, Copeland NG, & Jenkins NA. Mitf and Tfe3, two members of the Mitf-Tfe family of bHLH-Zip transcription factors, have important but functionally redundant roles in osteoclast development. *Proceedings Of The National Academy Of Sciences Of The United States Of Ame.* 2002; 99(7), 4477-4482.

Strähle, U., and P. Blader. Early Neurogenesis in the Zebrafish Embryo. *FASEB Journal: Official Publication of the Federation of American Societies for Experimental Biology* 8, no. 10 (1994): 692-8.

Sturm RA, Frudakis TN. Eye colour: Portals into pigmentation genes and ancestry. *Trends in Genetics.* 2004; 20(8):327-332.

Tachibana M, Perez-Jurado L, Nakayama A, et al. Cloning of MITF, the human homolog of the mouse microphthalmia gene and assignment to chromosome 3p14.1-p12.3. *Human molecular genetics.* 1994; 3(4):553-557.

Talbot JC, Amacher SL. A streamlined CRISPR pipeline to reliably generate zebrafish frameshifting alleles. *Zebrafish.* 2014; 11(6):583.

Theveneau E, Mayor R. Neural crest delamination and migration: From epithelium-to-mesenchyme transition to collective cell migration. *Dev Biol.* 2012; 366(1):34-54.

Verma AS, Fitzpatrick DR. Anophthalmia and microphthalmia. *Orphanet journal of rare diseases.* 2007; 2:47-47.

Wang Q, Fang W, Krupinski J, Kumar S, Slevin M, Kumar P. Pax genes in embryogenesis and oncogenesis. *J Cell Mol Med.* 2008; 12(6a):2281-2294.

Wasmeier C, Hume AN, Bolasco G, Seabra MC. Melanosomes at a glance. *J Cell Sci.* 2008; 121(24):3995.

Watanabe A, Takeda K, Ploplis B, Tachibana M. Epistatic relationship between waardenburg syndrome genes MITF and PAX3. *Nat Genet.* 1998; 18(3):283-286.

Yasumoto K, Shibahara S. Molecular cloning of cDNA encoding a human TFEC isoform, a newly identified transcriptional regulator. *Biochimica et biophysica acta.* 1997; 1353(1):23-31.

Zhao G, Zhao Q, Zhou X, Mattei MG, Decrombrugge B. Tfec, a basic helix-loop-helix protein, forms heterodimers with tfe3 and inhibits tfe3-dependent transcription activation. *Mol Cell Biol.* 1993; 13(8):4505-4512.

Zou J, Lathrop KL, Sun M, Wei X. Intact retinal pigment epithelium maintained by nok is essential for retinal epithelial polarity and cellular patterning in zebrafish. *The Journal of neuroscience : the official journal of the Society for Neuroscience.* 2008; 28(50):13684.

## **VITA**

Samantha Ashley Spencer was born on January 26<sup>th</sup>, 1991 in Richmond, Virginia. She received her Girl Scout Gold Award and graduated from the Mathematics and Science High School at Clover Hill in 2009. She graduated from Virginia Commonwealth University magna cum laude in 2013 with a Bachelor of Science in Forensic Science and minors in Biology and Chemistry.